

Digital Microwave Transmission Tests at the Pacific Missile Test Center, Pt. Mugu, California

R.W. Hubbard



U.S. DEPARTMENT OF COMMERCE
Malcom Baldrige, Secretary

Susan G. Stuebing, Acting Assistant Secretary
for Communications and Information

June 1983

Disclaimer

Certain commercial equipment, instruments, or materials are identified in this paper to specify adequately the experimental procedure. In no case does such identification imply recommendation or endorsement by the National Telecommunications and Information Administration, nor does it imply that the material or equipment identified is necessarily the best available for the purpose.

TABLE OF CONTENTS

	Page
LIST OF FIGURES	v
LIST OF TABLES	vi
ABSTRACT	1
1. INTRODUCTION AND OBJECTIVES	1
2. BACKGROUND	2
3. EXPERIMENT PLAN	4
3.1 Measurement Parameters	4
3.2 Link Configuration	4
3.3 BER and Burst Error Measurement	5
3.4 Adaptive Equalizer Control Voltages	6
3.5 RSL Records	6
3.6 PN Channel Probe	7
3.7 Angle Diversity Measurements	9
4. DATA ACQUISITION SYSTEMS	10
4.1 Digital Radio Performance Data	12
4.2 PN Probe and Other Data	14
5. DATA FORMATTING AND PROCESSING METHODS	15
6. PRELIMINARY RESULTS AND DISCUSSION	23
7. SUMMARY AND CONCLUSIONS	54
8. ACKNOWLEDGEMENTS	56
9. REFERENCES	58
APPENDIX	59

LIST OF FIGURES

	Page
Figure 1. Block diagram of the digital data acquisition system used in the radio experiment.	11
Figure 2. An example of the terminal/printer record from the digital data acquisition system. Periods between entries greater than 73 s (indicated by the arrows) show the times when error data were recorded on the magnetic tape.	17
Figure 3. An example of one 5 s data record read from the digital magnetic tape. The four independent data blocks are numbered in the figure; their content is described in the text.	22
Figure 4. The modified refractivity profile and resultant ray-trace cross section for the LP-SNI link on 7 August 1981.	25
Figure 5. The ray-trace cross section for propagation in a standard atmosphere over the LP-SNI link.	26
Figure 6. Refractive index profiles measured at Point Mugu on 18 August 1981.	32
Figure 7. Refractive index profiles measured at San Nicolas Island (SNI) on 18 August 1981.	33
Figure 8. Refractive index profiles measured at Point Mugu (PM) and San Nicolas Island (SNI) on 19 August 1981.	35
Figure 9. Graphical correspondence between delay-spread measurements and the refractivity data on the LP-SNI link on 18 August 1981.	37
Figure 10. Graphical correspondence between delay-spread measurements and the refractivity data on the LP-SNI link on 19 August 1981.	40
Figure 11. Refractive index profiles measured at Point Mugu (PM) on 1-2 September 1981.	41
Figure 12. The modified refractivity profile and the resultant ray-trace cross section for the LP-SNI link on 2 September 1981.	42
Figure 13. The theoretical frequency transfer function of the transmission channel for the multipath conditions on 1 September 1981. The illustration applies to the nominal multipath delay of 4 ns, measured during the interval of the data presented in Table 7.	46
Figure 14. A sample of the received signal spectra measured from both radios during the interval of test data given in Table 7.	48
Figure 15. Results of special nondiversity performance measurements performed on 2 September 1981.	50
Figure 16. An example of the spectral distortions caused by multipath activity during the special tests conducted on 2 September 1981. The spectral functions were recorded at 1 s intervals.	51

LIST OF FIGURES (Cont.)

	Page
Figure 17. A sample of the received signal spectra measured from both radios during the nondiversity test on the upper antenna (Figure 15). Note a gap in the record, indicating that the DRAMA radio registered no error or alarm data between 1850:57Z and 1851:17Z.	53
Figure A-1. An example of the errored-second performance data as it appears in the printer output record.	61

LIST OF TABLES

Table 1. LSI-11 Minicomputer System (CPU) Data	16
Table 2. Microwave Radio Performance Data	19
Table 3. Contents of the Octal Data from Figure 3	21
Table 4. Comparative Performance Data for 7 August 1981 (15-minute intervals)	27
Table 5. Comparative Performance Data for 7 August 1981 (1-minute intervals)	27
Table 6. PMTC Radio Performance Data, 18-20 August 1981	30
Table 7. Radio Performance Data on 1 September 1981	44
Table A-1. Digital Data Acquisition System - DRAMA Radio	60
Table A-2. DRAMA Radio Data Signals	62



DIGITAL MICROWAVE TRANSMISSION TESTS AT THE
PACIFIC MISSILE TEST CENTER,
PT. MUGU, CALIFORNIA

R.W. Hubbard*

This report describes an experiment designed to measure the performance of digital microwave radio systems in a line-of-sight (LOS) link that is subject to strong atmospheric multipath. It outlines the measurements made to characterize the propagation medium, the status of space-diversity receiver systems equipped with switched combiners, and the burst-error statistics caused by the multipath environment. The results presented in this report compare the performance of two radios, operating simultaneously in the same transmission channel. Detailed error distribution data have not yet been analyzed.

Key words: adaptive equalization; atmospheric multipath;
digital communications; impulse response

1. INTRODUCTION AND OBJECTIVES

This document presents some preliminary results of a test program designed to evaluate the performance of digital microwave systems in anomalous propagation conditions. The program was a joint effort of the Control Systems Development and Range Communications Divisions of the U.S. Navy Pacific Missile Test Center (PMTTC), and the Institute for Telecommunication Sciences (ITS), National Telecommunications and Information Administration (NTIA), U.S. Department of Commerce, Boulder, Colorado.

The objective of the program was to conduct and evaluate the results of a comprehensive experiment in which simultaneous measurements were made of the performance of a high bit-rate digital radio system and the propagation conditions in the radio transmission channel. The transmission channel was monitored with use of the ITS Pseudo-Random Noise (PN) Channel Probe (Linfield et al., 1976) in much the same manner as this system was applied to a previous experiment at PMTC (Hubbard, 1979). The performance of the radio system(s) was measured through use of a bit-error-rate (BER) instrument and an error analyzer, with emphasis placed on the distribution of bit-errors.

The anomalous propagation condition of interest is that of multipath, created by either refractive effects of the atmosphere, or superrefractive height profiles

*The author is with the Institute for Telecommunication Sciences, National Telecommunications and Information Administration, U.S. Department of Commerce, Boulder, Colorado 80303.

that produce strong ducting conditions within the channel. In order to determine the meteorological conditions for the channel, the Geophysics Division at PMTC supported this program with all appropriate data. These data consisted of at least two radiosonde observations each day, taken at both terminals of the test path. In addition, forecast statements relative to expected ducting and other pertinent weather features were issued daily by this department. The forecast memos were used to direct special features of the measurements as appropriate. The radiosonde data were compiled into refractive index profiles, and plotted by computer routines. The profile plots were made available to the experiment team within a short period of time after a radiosonde launch.

The combination of the impulse response and performance data in this program marked another "first" in the field of digital microwave performance tests. Earlier, ITS measurements demonstrated the catastrophic impact that atmospheric multipath can have on digital transmission [Dougherty and Hartman, 1977]. Many experimentors have reported performance measures on digital systems, with limited knowledge or observation of multipath phenomena. Others, including the ITS, have made significant measurements relative to digital microwave propagation parameters. These include impulse response and meteorological data. Rarely, however, have these two facets of digital communication experiments been performed simultaneously, particularly over the same transmission channel. A direct correlation of these data will provide new insight to performance criteria, and knowledge of adaptive techniques that will serve to improve the future performance of this very important communication technology. It is expected that the data will also be useful in enhancing analytical models for LOS digital systems.

2. BACKGROUND

Multipath in a microwave propagation path is a problem of growing concern to both military and commercial users. A significant body of performance measurements have been reported in the literature in the last few years. Examples of specific experiments are given by Anderson et al. (1978) and Barnett (1978). Both of these papers illustrate the degradation in performance due to multipath propagation. However, each experiment relied on only cursory observations of the multipath structure, derived from observing some characteristic of the received signal in the digital microwave system. No direct observation of the channel multipath was available, and no observations were made that could determine the origin or statistics of the multipath signals.

In preparing plans to convert their range communication systems (PMTC, 1976) to an all digital format in the future, the PMTC began to assess the potential

performance of these microwave systems with respect to their mission requirements. The multipath question was of paramount importance because of the known and persistent meteorological conditions that develop along the Southern California coast. The PMTC has maintained microwave propagation records for many years, and observed the multipath effects in their analog systems. The worst propagation periods usually occur when a marine layer of moist air develops offcoast, and causes a temperature inversion. This weather condition results in a superrefractive (often exceeding ducting conditions) layer in the propagation channel. The knowledge of these conditions prompted the PMTC to investigate the multipath problem in detail, prior to investing in any specific digital system. The ITS performed impulse response measurements over a 65 mi (104.6 km) overwater link between Laguna Peak (LP) at Point Mugu, and San Nicolas Island (SNI), to evaluate the multipath problem. These measurements were reported in the reference given previously (Hubbard, 1979). The PN probe signal was multiplexed onto the PMTC system at SNI, and the impulse response was simultaneously measured on both of the space diversity channels at LP. In addition, the error performance of the PN code used for the impulse response measurements was also monitored at LP. The PN probe was operated at 8.6 GHz. The PMTC microwave system was operating on 7.17 and 7.47 GHz.

Based on the results of the above experiment, it was concluded that a digital system operating with a mission bit-rate on the order of 50 Mb/s would perform adequately over this link, provided that space and frequency diversity and adaptive equalization were used to combat the multipath effects. Subsequently, the PMTC has purchased a commercial digital microwave system which operates in an 8-PSK mode at a T3 transmission rate of 44.736 Mb/s (2.25 bits/Hz). This system was installed on the LP-SNI link using space diversity reception and adaptive spectrum equalization, and was used in the test program reported here. The system was made available for experimental purposes for a period of about one year. This permitted measurements to be made through the most severe anomalous propagation periods, which are the summer and early fall months. Similar conditions usually develop on this path during December and January, but do not persist for long periods of time.

The specific measurements made during this experiment are outlined in the following sections. Initially, the measurements were made on the PMTC 44.736 Mb/s system. However, a second microwave system was added to the experiment at a later date. This was a prototype of the Digital Radio and Multiplex Acquisition (DRAMA) system under development by the military. This report presents the results of selected test periods where the performances of the two radios are compared. The

DRAMA tests have been reported separately¹. A complete report of the PMTC radio tests will be published at a later time.

3. EXPERIMENT PLAN

3.1 Measurement Parameters

This experiment included the following measurements, each of which is discussed independently in subsequent subsections.

1. BER and burst-error statistics of the mission bit-stream of the microwave radio.
2. Two control voltages developed by each adaptive equalizer unit in the two receiver channels of the PMTC digital radios. These signals are proportional to the "tilt" and "notch" gain function of the equalizers, and are thus a measure of the multipath effects in the signal pass-band of the receiver.
3. Received signal level (RSL) of each space diversity channel, from the two microwave receivers. In association with these measurements, the diversity switch status was also recorded, so that a record is maintained as to which diversity channel was selected for data reception. The RSL of the PN probe system was also recorded for frequency comparison.
4. Impulse response data of the propagation channel, including statistics of the frequency selective fading in the broadband spectrum of the PN probe system. The impulse response was measured on two diversity channels simultaneously.
5. Angle diversity measurements. These were conducted in a similar manner to that used in the earlier measurement on the PMTC link (Hubbard, 1979).

3.2 Link Configuration

The LP-SNI link was configured for measurements of the digital performance in one direction only; the transmitter terminal was located on SNI, and the receivers and data acquisition systems were located on LP. For all other instrumentation, including the PN probe, the transmitters were located at SNI, and the receiving equipment was located at LP.

The LP-SNI link is characterized as follows:

Site Elevation at LP: 1400 ft (426.7 m) above msl

Site Elevation at SNI: 912 ft (278 m) above msl

Length (over water): 65 mi (104.6 km)

¹Hubbard, R.W. (1982), Digital European backbone (DEB) stages II-IV, propagation dependent availability FOT&E report, ITS report to sponsor (distribution limited to U.S. Government Agencies only), October.

Transmitter Antenna: 10 ft (3.05 m) paraboloid; 70 ft (21.3 m) above ground

Receiving Antennas: 10 ft (3.05 m) paraboloids; 30 ft (9 m) and 120 ft (36.6 m) above ground

Vertical Diversity Spacing: 90 ft (27.4 m)

Antenna Gains at 7350 MHz: 44 dB

The frequency assignments for the microwave systems are as follows:

PMTC Analog System: 7170 MHz and 7470 MHz

PMTC Digital System: 7350 MHz and 7800 MHz

DRAMA Prototype: 8140 MHz

ITS PN Channel Probe: 8600 MHz

3.3 BER and Burst Error Measurement

The BER and burst-error measurements were made using commercial instruments manufactured by Tau-Tron, Inc. The basic error detector was a model PTS-107. This system uses a PN sequence as a test signal, which is selectable in length from (2^7-1) to $(2^{20}-1)$. A $(2^{15}-1)$ sequence was transmitted at a T-3 rate of 44.736 Mb/s. The error analyzer was set to match the code length and clock rate at the transmitter. The output signal of the PTS-107 was a serial pulse for every bit in error in the detection process. The error-pulse stream was fed to a companion instrument, an MK-4 error analyzer. This instrument provides the following information:

1. Number of error-free sync periods. (This statistic was tabulated in fixed time intervals for long error-free periods; see Section 4.1.)
2. Number of error-free bits from the last sync signal to the first error burst.
3. Length of each burst of errors.
4. Number of bits in error in each burst.

Two parameters were selectable for the above burst-error analysis. The first was the length of a coarse sync period, and the second was the length of the error-free gap between bursts. The sync period was chosen for an unambiguous result (see Section 4.1), and the error-free gap may be selected within the binary range of 32 to 256 bits. The smallest error-gap of 32 bits was initially selected. However, this value was changed during the experiment to the maximum of 256 bits, because of the severity of the error data.

The data output of the burst-error system is composed of 10 BCD digits, containing the burst statistics noted above. These data were recorded in a digital data acquisition system (see Section 4). No direct record of the BER was included

in the digital records. However, this parameter was recorded on an auxiliary thermal line printer for a permanent record and on-site review. It should also be noted that BER (for any selected period of time) may be developed from the analysis procedures used on the digital burst-error data.

All recorded data were time-tagged with an appropriate clock, as described under the description for the data acquisition systems (Section 4). This assured proper time synchronization of all data records for correlation analyses.

3.4 Adaptive Equalizer Control Voltages

Two control voltages from each of the two (diversity) receivers in the PMTC digital radios were recorded. These control voltages indicate the adaptive gain function in the equalizers for correcting the multipath "tilt" within the data bandwidth, and the effects of a multipath "notch" when it appears near the band center. Each of these signals is an analog output of the adaptive equalizers. They were A/D converted at a rate of 10 samples per second, and recorded in the digital acquisition system. Calibration of these signals was performed initially by using a special test unit developed by the radio manufacturer.

The equalizer data provided a permanent record of the following phenomena:

- a. Relative position and depth of a multipath notch in the transmission channel; i.e., the encroachment of a frequency selective fade on the signal pass-band, and the position (either above or below) the center frequency.
- b. Depth of a frequency selective notch when it appears near the band center of the signal spectrum.

3.5 RSL Records

The received signal level (RSL) of each of the digital diversity receivers was recorded. The two analog signals were A/D sampled at a rate of 10 samples/s, and recorded in the digital acquisition system.

Calibration of the RSL signals was performed by using a stable signal generator with a precision attenuator. Calibrations were performed as required, so that a valid calibration was available for each data tape. The appropriate calibration data were retained in storage in the data system for regular data runs. For any special runs, such as those outlined below for diversity etc., a special calibration was made.

3.6 PN Channel Probe

As noted previously, the ITS PN channel probe was used in the experiment to measure and record the impulse response of the propagation channel. This system was multiplexed onto the existing PMTC microwave transmission lines. The multiplexers were furnished by ITS. They are designed to pass (with <1 dB insertion loss) the PMTC operating frequencies in the range of 7.15 to 7.90 GHz through the primary port. The second port accommodated the PN probe signal at 8.6 GHz, with a pass band of ± 200 MHz. The isolation between these ports is in excess of 50 dB. The use of this multiplex arrangement permitted the impulse response to be measured over precisely the same propagation path as the digital radio transmission.

The channel probe uses a PN code length of 511 bits (2^9-1), clocked at rate of 150 MHz. This permits a multipath delay resolution (without overlap) of approximately 6.67 ns. The actual resolution is however, on the order of 1 ns in most instances. The system employs a dual receiver, so that simultaneous data may be obtained on diversity paths. Four analog data signals are available from each receiver channel as follows:

1. Co-phase impulse [$h_r(\tau)$]
2. Quadrature-phase impulse [$h_i(\tau)$]
3. Power impulse function [$\Sigma(\cdot)^2$]
4. RSL (power level detector on 600 MHz IF).

The PN probe develops the impulse response measurement using a correlation detection process in the receiver. This technique provides a time-bandwidth trade-off in comparison with rf impulse measurements. Since most propagation channels change characteristics relatively slowly, the PN probe has been configured to develop the response at a data rate from 1 impulse/s to 10 impulses/s. The 1 impulse/s rate for line-of-sight (LOS) microwave links has proven adequate in most of the previous experiments, and was used predominately in this experiment. The total delay time (window) possible from the measurement is 3.4 μ s for the specified code length and clock rate. However, the data of interest in a LOS circuit is generally confined to a few ns.

The impulse response data gathered during the early part of the PMTC test program were recorded separately on analog magnetic tape. The local PMTC IRIG B time code (used to synchronize all of the data, as explained in Section 4) was also recorded on the analog tapes. In this fashion, the analog tape records can be completely synchronous with the digital tape records of other data.

Later, with the addition of the DRAMA radio to the experiment (under sponsorship of the U.S. Air Force), a second digital data acquisition system was implemented. At this time, the impulse response data were also recorded in a digital format. The sampling rate for these data was 2 kHz but the sampling range was restricted to approximately 40 samples. The equivalent time resolution was approximately 2 ns/sample in the recorded response, which permitted multipath delay measurements to a maximum of 80 ns.

The data recorded in the analog system was played-back on-site for a review of events that occurred during periods when the receiving site was unattended.

In addition to the above signals, two additional data sources were derived from the PN probe. The first was a measure of the BER of the test signal used in the PN probe. The 150 Mb/s data stream was detected in one channel of the receiver only, and was fed to the input of a commercial error detector. The error performance on this signal was in direct time relationship to the frequency selective fading caused by multipath in the channel, and could be visually correlated with the corresponding impulse response. These data were used as an on-site monitor for path conditions, and were not recorded for analysis.

Since frequency selective fading will affect the different operating frequencies at different times, the BER data from the probe measurement was used for comparison with the short term effects measured on the PMTC digital data. This visual monitor technique permitted on-site observation of multipath effects, and they could be traced across a wide range of microwave transmission frequencies; those listed in Section 3.2. When the DRAMA prototype radio was added to the experiment, a total of five different transmission frequencies was observed, ranging from 7.17 GHz to 8.6 GHz. This data base provided new insight to the correlation properties of multipath effects.

Another data source from the probe system was implemented to monitor continuously the band-edge effects on the transmission during multipath activity. For example, the delay time of a multipath component will change over a period of time. This will cause a number of frequency-selective notches to move rapidly through the signal pass-band. It was expected that this phenomenon would be the predominant cause of any burst-error type performance, and thus the band-edge signals were recorded so that they could be directly correlated with the burst-error measurement. The data were recorded as one of the analog inputs to the digital data system. The actual signal format is explained below.

To develop the band-edge signals, the 150 MHz clock frequency used in the PN probe was inserted (amplitude modulated) onto the transmitted signal. The PN transmitted (bi-phase) spectrum follows the $(\sin x/x)^2$ power law. For the biphasic signal, a spectral null occurs at points ± 150 MHz from the center frequency. The added clock frequency thus appears as a spectral line at these null points, and does not cause any interference effects to either the BER or impulse response measurements. The amplitude modulated spectral lines thus appear in the received IF spectrum at the bi-phase band edges at 450 MHz and 750 MHz (IF = 600 MHz). These two spectral lines were filtered and fed to two independent amplifiers for separate measurement. Tilt across the transmission BW is registered by the difference in magnitude of these detected signals. Any rapid movement of frequency selective fades (due to multipath with changing delay time) was detected by the fading character of these signals.

The measurement of prime importance is the relative amplitudes of the two inserted signals. Thus, in the recording of these data, the difference between the two detected magnitudes was actually recorded. One signal was inverted and algebraically combined with the second signal. In this manner, the polarity of the combined (recorded) signal indicates on which side of the signal spectrum a multipath notch has impinged. In addition, a cyclic pattern to the signal indicates the motion of a notch completely through the signal pass-band, and the phase or timing of the notch movement (+ or - on the frequency axis). This data signal was handled as an additional analog output from the PN probe; i.e., it was sampled in the A/D conversion interface, and recorded on the digital data records. This signal is primarily intended for use in developing the time statistics of the frequency selective fading.

There was no direct calibration of the individual magnitudes of the band-edge signal. However, the differential signal was calibrated by using precision attenuators to measure the tilt and notch variations in dB. Other data, such as described in Section 3.4, provide similar frequency selective fade information at a different rf carrier, and a correlation between the two sets of data can be performed in the data analysis procedures.

3.7 Angle Diversity Measurements

The angle diversity measurements described by Hubbard (1979) on the SNI-LP link were continued during this experiment. A separate dual receiver (furnished by ITS) was used at LP to monitor one of the PMTC analog radio frequencies. The receiver is

tuneable over the range 7.1 to 8.4 GHz, and it provides two independent log-linear RSL outputs for recording. Two 1.2-m (4-ft) parabolic antennas were previously mounted on the LP tower for these measurements. One antenna was aligned to an on-path elevation. The other was tilted slightly in elevation to provide the angle-of-arrival diversity.

The angle diversity measurements were performed only on an occasional basis. Data were recorded on a paper strip-chart recorder for visual on-site monitoring. Periodically, these data signals were recorded on both digital and analog magnetic tape for later analysis in the ITS laboratories. The objective of these measurements is to determine the feasibility of angle diversity reception as an adaptive technique to specific types of multipath in a digital transmission channel. When these measurements were performed, certain periods of time were devoted to measuring the impulse response of the channel directly over the angle diversity paths. This was accomplished by removing the input lines to the PN probe receiver from the PMTC antennas, and connecting them to the two angle diversity antennas. Specific times and duration of these measurements were determined on-site, based on channel conditions and system performance parameters.

Further details of this form of angle diversity, and performance improvement may be found in the report by Hartman and Smith (1975).

4. DATA ACQUISITION SYSTEMS

Three data acquisition systems were used in this experiment; two digital systems and one analog system.

The two digital systems are fundamentally the same, each configured for the assimilation of analog data through an appropriate A/D conversion interface. Both systems contained the appropriate interface cards for a BCD or ASCII coded digital data input. The BCD interface was used for the burst-error analyzer noted in Section 3.3. The ASCII interface was provided in the second system to accommodate an errored-second instrument used in the DRAMA radio measurements (see Appendix).

The heart of each data system was a minicomputer CPU (DEC/LSI-11). Each had a keyboard for operator interface and control, and a dual floppy-disc for data storage and for program development/operation. The primary data storage medium on each system was digital magnetic tape. Both systems were capable of 1600 bpi, phase encoded recording. A basic block diagram of the systems is shown in Figure 1.

Each of the digital systems contained an integral calendar and time of day clock. These were synchronized with PMTC range time, so that each data record was

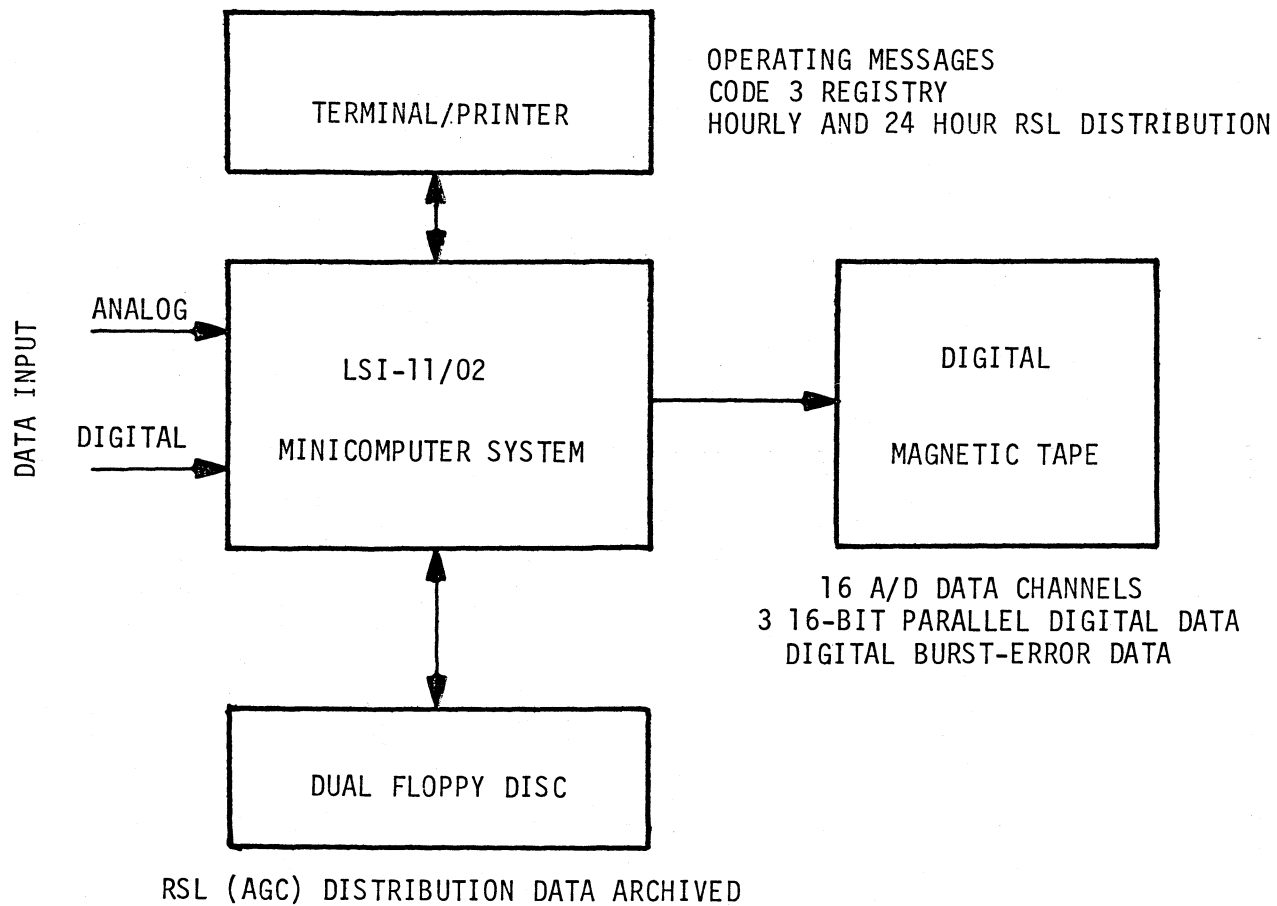


Figure 1. Block diagram of the digital data acquisition system used in the radio experiment.

precisely time-tagged to the same reading. The synchronizing source was the IRIG B time code distributed to various sites at PMTC.

The analog data system was composed of magnetic tape recorders, strip chart recorders, thermal printers, storage oscilloscope with camera, and spectrum analyzers. Some of these instruments and their application have been mentioned previously. Details of the data formats and applications of these instruments are provided in the following subsections, interspersed with the corresponding details for the digital acquisition systems.

4.1 Digital Radio Performance Data

The primary digital radio performance parameters and signals were recorded in the all-digital acquisition systems. The analog signals described in Sections 3.4 and 3.5, were interfaced to the digital data acquisition system through 12 bit A/D converter cards with an integral multiplexer. The sampling rate ranged from 10 to 2000 samples/s, based on the Nyquist requirement for each of the analog signals. These data were temporarily stored in the CPU for later transfer to digital magnetic tape. The basic data format was designed first to compile the A/D (analog) data into a block, and then to follow this with the burst-error data described below. Each record file was headed by a time-of-day entry, which also serves as a file identifier.

The burst-error data for the PMTC radio consisted of those entries noted in Section 3.3. They were formatted into a 10 digit BCD arrangement within the MK-4 instrument. The data were compiled into a first-in first-out (FIFO) type buffer, which is 256 data words in depth. At the maximum (estimated) rate of burst-error activity (4 k bytes/s), this FIFO buffer was capable of storing approximately 250 ms of data. While these data were accumulating, the digital acquisition system was recording the analog signal samples. Following this, the burst-error FIFO contents were read and recorded into the same record file on digital tape. A record file consisted of 5 s of data, timed by the internal data system clock.

The burst-error data acquisition system was initiated by the first error detected in any sequence of error activity. During periods of error-free operation, the digital system did not record data. However, the RSL data continued to be read into the system, and rather than record the signals on the digital tape, they were compiled into cumulative distributions for periods of 1 hour and 24 hours. These distributions were recorded on floppy-discs in the computer system.

The first register in the MK-4 system counts the number of error-free coarse sync periods, where the coarse sync may be arbitrary in period, within specified

limits. For this experiment, the course sync period was derived from the PN code-sync signal so that an unambiguous record of the error-free clock periods to the first error following a sync pulse could be maintained. The actual value was chosen to correspond with the instrument characteristic that all of the counters would overflow with a count in excess of 10^5 . For example, in a burst-error situation, in order to keep the count of error-free bits from any sync pulse (or previous burst) from becoming ambiguous (prevent counter overflow), the coarse sync could not exceed the product of the bit period ($0.02235 \mu\text{s}$ for 44.736 Mb/s) times 10^5 . A coarse sync period of less than 2.235 ms meets this criterion.

The coarse sync period used for the tests was derived directly from the PN word sync signal (from the PTS-107 Error Detector Receiver). The following are the specifications selected for the tests:

PN Code Length: $(2^{15}-1) = 32,767$ bits

Bit Rate: 44.736 Mb/s

Bit Time: $1/44.736 \mu\text{s} = 0.022353362 \mu\text{s}$

PN Sync Period: $32,767 \times 0.022353362 = 0.732452611 \text{ ms}$

(Coarse Sync for MK-4 Burst Error Analyzer).

During error-free periods of performance, the burst-error analyzer continued to register the number of error-free coarse sync periods. Again, this counter overflow value is 10^5 . Thus, to reach an overflow count, the total time lapse was approximately:

$$0.73245 \text{ ms} \times 10^5 = 73.245 \text{ s}.$$

The output of the burst error analyzer is a data "Code 3" for a sync counter overflow. This output was tabulated on the terminal printer of the data system for each of the above intervals during error-free periods. A real time clock entry was also made on the printer to assure that these error-free data periods comprised a continuous record of performance. This record also provided a check of proper systems performance during the error-free periods of time. We reemphasize the fact that the digital data acquisition system is idle during error-free periods, and did not assimilate the error-free coarse sync periods.

Another data entry into the digital system was the switch status of the diversity digital radio. This was a 1-bit entry, which was coded to identify which diversity receiver was in the selected operating mode during any data entry. Other status and alarm signals from the digital receivers were recorded in the same manner, using a 16-bit interface (I/O) board in the computer acquisition system. The board was read every 0.1 s during a data record.

The IF signal spectra from the PMTC digital radio were recorded on analog magnetic tape, along with the PN probe data noted below in Section 4.2. The vertical output signals from the two spectrum analyzers were fed to an analog combining circuit, and the two spectral functions were recorded on a single track of the tape. A control circuit was operated synchronously with the PN probe timing signal so that the output spectrum from one receiver followed that of the other in time. Thus the spectra information could be recorded on a single tape track. To accomplish this, one spectrum analyzer was set to trigger on the return trace of the first instrument. Both spectral functions, one for each diversity receiver, were recorded for each second, along with the channel impulse function.

4.2 PN Probe and Other Data

The PN probe impulse response data were recorded in the digital acquisition system noted at the beginning of this section. The power impulse as well as the co- and quad- phase functions from each receiver channel were recorded in the digital mode, where each signal was sampled in the A/D interface as noted in Section 3.6. The RSL data and the band-edge signal from the probe receiver were also recorded in the digital system.

An analog tape recorder was used as a back-up data system, and as an on-site playback system to permit data monitoring. The analog records also contain the power impulse response from each diversity channel, the RSL record for each channel, a sync signal for the impulse data, the band-edge differential signal, and the IRIG B time code. These data were recorded on an as-needed basis, rather than continuously. The tape recorder was used during only the most significant events of the experiment, and during periods when the receiving site was left unmanned.

Other on-site instruments included a storage-type oscilloscope and camera, which was used to monitor the impulse response data. The camera was useful for providing quick and permanent records of unusual response functions, or to provide a time-sequence record of the dynamics of the response. The BER measurement made on the PN probe signal was recorded on a thermal line printer. These data were not permanently retained for analyses. They were used primarily for on-site monitor purposes only.

The analog tape recorder was also used periodically to record the signals from the angle diversity tests.

5. DATA FORMATTING AND PROCESSING METHODS

A complete list of all of the signals recorded for the digital radio performance tests are shown in Table 1. A description of each and the purpose for the record was given above in Section 4. In this section, we will describe the formatting of these data, and outline the analysis procedures.

As stated in the previous section, any long periods of error-free performance for the digital radio was registered on the terminal/printer of the data acquisition system. An example of these entries is shown in Figure 2. A "Code 3" on the record corresponds to an error-free period, counted as the number of error-free sync periods as noted in Section 3.3. An error-free sync period and its overflow condition was defined in Section 4.1. Thus, each Code 3 message on the terminal represents 73 s of error-free data. Figure 2 shows a continuum of these entries, interspersed with periods of error data. The periods of error are indicated on the figure with the drafted arrows, along with the duration of the recorded data on magnetic tape. Figure 2 also shows a typical message that was printed on the terminal for information to the system operator. In this instance, an end-of-tape message is seen, and the record shows that a new tape was mounted and the data system restarted with a loss of data of approximately 3 minutes. Each entry is identified with the date (month/day) followed by the time of the entry (Zulu).

During error data, two distinct protocols were used to direct the computer system to transfer all buffered data to the magnetic tape. These were:

1. any time that error data were received in the storage buffer; and
2. any change in the receiver status/alarm signals at the 0.1 s intervals.

Thus, at any time that either of the above conditions was met, the entire data file in the storage buffers was written to the magnetic tape. The buffers contained 5 s of data, and these were recorded as a single record. A data record is composed of four distinct blocks, organized as follows:

- 1 - Date and time (Z), which serves to identify each record. Number of data entries in block No. 4.
- 2 - A/D data (16 x 50 grid)
- 3 - Digital receiver status (100 ms intervals)
- 4 - Digital burst-error data (100 ms timing marks)

A typical example of one 5 s data record, as read from the magnetic tape, is shown in Figure 3. The data blocks listed above are numbered accordingly in this figure.

Table 1. LSI-11 Minicomputer System (CPU) Data

<u>DATA SOURCE</u>	<u>SIGNAL DESCRIPTION</u>	<u>DATA RECORD</u>
44.7 MB/S DIGITAL RADIO (MDR-8)	ANALOG	
	1. RSL CHAN A (LOWER ANTENNA)	DIGITAL MAG TAPE
	2. RSL CHAN B (UPPER ANTENNA)	
	3. AE SLOPE CHAN A	
	4. AE SLOPE CHAN B	
	5. AE NOTCH CHAN A	
	6. AE NOTCH CHAN B	
	7. RAIL CLOCK REFERENCE	
	8. RAIL CLOCK DELAY	
9. BIT ALIGNMENT		
	DIGITAL STATUS	
	1. REC IN SERVICE	DIGITAL MAG TAPE
	2. AGC/AE OFF NORMAL A	
	3. AGC/AE OFF NORMAL B	
	4. LOSS OF FRAME A	
	5. LOSS OF FRAME B	
	6. BER 10^{-7} A	
	7. BER 10^{-7} B	
	8. BER 10^{-2} A	
	9. BER 10^{-2} B	
10. CONTROL SWITCH OFF NORMAL		
MK-4 BURST ERROR ANALYZER	DIGITAL ERROR DATA	
	1. BURST ERROR STATISTICS	DIGITAL MAG TAPE
PN CHANNEL PROBE	2. ERROR FREE SYNC PERIODS	TERMINAL PRINTER
	1. RSL CHAN A *	DIGITAL MAG TAPE
	2. RSL CHAN B *	
3. TILT/NOTCH SIGNAL *		
PMTIC ANGLE DIVERSITY	1. RSL CHAN 1 *	DIGITAL MAG TAPE
	2. RSL CHAN 2 *	

*PARALLEL DATA ON ANALOG MAGNETIC TAPE.

```

CODE 3 12/22 7: 8: 6
CODE 3 12/22 7: 8: 6
CODE 3 12/22 7: 9:24
CODE 3 12/22 7:10:38
CODE 3 12/22 7:11:51 → 2:16 → MAGNETIC TAPE DATA ENTRIES
CODE 3 12/22 7:14: 7
CODE 3 12/22 7:15:20 → 2:02
CODE 3 12/22 7:17:22 → 3:10
CODE 3 12/22 7:20:32
WAIT FOR TAPE TO REWIND
THEN MOUNT NEW TAPE & HIT RETURN KEY TO RESTART PROGRAM
PAUSE ---

```

```

CODE 3 12/22 7:23:48 → 2:02
CODE 3 12/22 7:25:50
CODE 3 12/22 7:27: 3 → 1:38
CODE 3 12/22 7:28:41
CODE 3 12/22 7:29:55
CODE 3 12/22 7:31: 8
CODE 3 12/22 7:32:21
CODE 3 12/22 7:33:34
CODE 3 12/22 7:34:48
CODE 3 12/22 7:36: 1
CODE 3 12/22 7:37:14
CODE 3 12/22 7:38:27
CODE 3 12/22 7:39:41
CODE 3 12/22 7:40:54
CODE 3 12/22 7:42: 7
CODE 3 12/22 7:43:20
CODE 3 12/22 7:44:34
CODE 3 12/22 7:45:47
CODE 3 12/22 7:47: 0
CODE 3 12/22 7:48:13
CODE 3 12/22 7:49:27
CODE 3 12/22 7:50:40
CODE 3 12/22 7:51:53
CODE 3 12/22 7:53: 6
CODE 3 12/22 7:54:20 → 1:39
CODE 3 12/22 7:55:59
CODE 3 12/22 7:57:12
CODE 3 12/22 7:58:25
CODE 3 12/22 7:59:38

```

Figure 2. An example of the terminal/printer record from the digital data acquisition system. Periods between entries greater than 73 s (indicated by the arrows) show the times when error data were recorded on the magnetic tape.

The A/D records in block No. 2 are for the 16 channels from left to right, and the entries are printed in decimal values. Block No. 3 contains the receiver status/alarm data, entered in an octal code for the 16 bits of information. The data in block No. 4 are the burst-error data as recorded from the MK-4 instrument. The entry "40" represents the 100 ms timing marks within the block, during which no error or alarm data were received. Starting after the 38th time mark (3.8 s after the record time in block No. 1) the data indicate that either a burst of error or a receiver status signal was received. The data entries are treated in groups of three octal numbers, which show the digital status of all three I/O boards in this block. An interpretation of some of these octal entries is given later in this section.

Details of the error performance data are given in Table 2, where the Code numbers are identified (including the Code 3 discussed above). The distribution data accompanying each Code is also given in Table 2.

A complete analysis of the recorded data has not been made at this writing. Some analyses are in process by PMTC, and a detailed analysis is anticipated as a new project at ITS. This section is provided merely to indicate the manner in which the data were formatted, and the methods for compiling the results. It can be seen, for example, that a complete distribution of error-free time can be readily compiled by totalizing the time for Code 3 entries. In like manner, the following are examples of the statistical data that will be developed in future analyses from the error data:

1. distribution of the lengths of error-free sync periods (from Code 0 and Code 1 data);
2. distribution of error-free gaps (Code 1 and Code 2 data);
3. distribution of error-bursts;
4. distribution of the number of subsequent error bursts;
5. distribution of the error-free periods between bursts (>gap length);
6. distribution of error-burst lengths;
7. distribution of the number of errors within a burst;
8. distribution of the ratio of burst length to error count within a burst; and
9. distribution of sync-loss counts and duration.

The above list is not exhaustive, but it includes the major distributions that can be readily obtained with the proper search program of the data tapes. Since these data are essentially synchronous with the propagation-oriented data, the potential

Table 2. Microwave Radio Performance Data

PN TEST CODE = $(2^{15}-1) = 32,767$ BITS/SEQUENCE

TRANSMISSION RATE = 44.736 MB/S

BIT PERIOD (T) = $1/44.736 = .022353$ --MICROSECONDS

PN SYNC PERIOD = $32,767 \times T = 732.45$ --MICROSECONDS

10^5 SYNC PERIODS = 73.245--SECONDS

ERROR GAP LENGTH = 256 BITS

TAU TRON MK-4 BURST ERROR ANALYZER DATA:

CODE \emptyset -- FIRST BURST AFTER A NUMBER OF ERROR-FREE SYNC PERIODS
COUNTS NUMBER OF ERROR-FREE SYNC PERIODS

CODE 1 -- FIRST ERROR-BURST DISTRIBUTION
COUNTS NO. OF BITS FROM LAST SYNC TO FIRST ERROR
COUNTS NO. OF BITS IN ERROR
COUNTS THE LENGTH OF THE BURST IN NO. OF BITS

CODE 2 -- SECOND (OR SUBSEQUENT) BURST DISTRIBUTION WITHIN
A SYNC PERIOD
SUBSEQUENT BURST DECLARED IF GAP LENGTH IS EXCEEDED
DISTRIBUTION DATA SAME AS CODE 1

CODE 3 -- SYNC COUNTER HAS REACHED 10^5 ERROR-FREE SYNC PERIODS
CODE 3 MESSAGE AND DATE/TIME LINE ARE PRINTED ON THE
DATA SYSTEM TERMINAL

CODE 4,5,
6, 7 -- SAME AS CODES $\emptyset, 1, 2, 3$ RESPECTIVELY, INDICATING
THAT THE MK-4 FIFO BUFFER IS FULL

for meaningful studies of the correspondence between these data is quite high. As one example, consider the correlation between spectral distortions measured by the "tilt" and "notch" signals in the A/D data bank, and the detailed error analysis listed above. The results will illustrate what the most important performance parameters are and should lead to conclusions toward methods of improving the performance. This aspect, coupled with an evaluation of the meteorological description of the transmission channel, offers an approach to the analysis that encompasses all of the system and propagation variables.

The status/alarm data from the experiment expand the concepts noted above. For example, distributions of the diversity switching and duration of time that a given receiver is selected are also available from the data. Referring to Table 1, other significant parameters for analyses are:

1. Rail clock statistics
2. Bit alignment characteristics
3. BER alarm distribution for independent diversity receivers
4. Loss of frame data for each diversity receiver.

As an aid to the reader, we present in Table 3 some examples of how the recorded data (octal words) are decoded to yield the information discussed above. The particular entries refer to the raw data that are shown in the playback record of Figure 3. Those that are included in this table are underlined in Figure 3.

The top half of the table illustrates the decoded status/alarm signals in data block No. 3. We note that the first word in the block indicates a Code 1, which does not change until index word No. 40. This is merely an indication that the last MK-4 registry was a Code 1 from some previous data block. The remainder of the octal code word indicates the status/alarm signal states for the diversity receivers. These are delineated in the table, and they indicate (1) periods of excessive BER and loss of frame in Receiver A; (2) Receiver B as the selected operational unit; and (3) normal conditions for Receiver B. In this data block, each index is registered at 100-ms intervals. Thus, the time at which changes occur are known to within that interval from the record time shown in data block No. 1.

The first status entry in which error data were registered is in index No. 40, where a Code 0 is seen. However, examination of data block No. 4 shows that the error burst actually started after index No. 38 (between No. 38 and No. 39). A total of four MK-4 entries were recorded in this 100-ms interval. They are shown with the decoded contents in the lower half of Table 3. It should be kept in mind that these entries are taken as rapidly as they are generated in the MK-4 FIFO, and are not interrogated by the computer system as are those entries of data block No. 3.

Table 3. Contents of the Octal Data From Figure 3

DIGITAL DATA DECODE: 12/22/80 7:24:37 Z

<u>INDEX NO.</u>	<u>OCTAL CODE</u>	<u>STATUS</u>
1-16	177706	CODE 1, REC B, NORMAL OPERATION
17-19	152706	CODE 1, REC B, NORMAL OPERATION REC A BER 10^{-7} and 10^{-2} REC A LOSS OF FRAME
20-22	157706	CODE 1, REC B, NORMAL OPERATION REC A BER 10^{-7}
23-27	152706	AS ABOVE
28-35	157706	AS ABOVE
36-38	177706	AS ABOVE
39	157706	AS ABOVE
40	156702	CODE \emptyset , REC B, NORMAL OPERATION REC A BER $>10^{-7}$ and 10^{-2}
41-33	152706	AS ABOVE
45	156706	CODE 1, REC B REC A BER $>10^{-7}$ and 10^{-2}
46-50	157706	CODE 1, REC B REC A BER $>10^{-7}$
<u>BURST ERROR DATA DECODE FOLLOWING INDEX NO. 38</u>		
38+	177302	CODE \emptyset , REC A, NORMAL STATUS
	177020	BURST BEGAN AFTER 10×10^3 ERROR FREE SYNC PERIODS (NO MEANING)
	177306	CODE 1, REC A, NORMAL STATUS
	006027	BURST BEGAN 17×10^3 BITS AFTER LAST SYNC PULSE
	021421	BURST STATISTIC: 11 ERRORS IN LENGTH 23 BITS
	177302	CODE \emptyset , REC A, NORMAL STATUS
	171043	BURST BEGAN AFTER 23×10^0 ERROR FREE SYNC PERIODS
	177777	(NO MEANING)
	157706	CODE 1, REC B, REC A BER $>10^{-7}$
	006047	BURST BEGAN 27×10^3 BITS AFTER LAST SYNC PULSE
	032030	BURST STATISTIC: 18 ERRORS IN LENGTH 34 BITS

The sequence of events during the time between the 38th and 39th index can be gleaned from the decoded entries in Table 3 (lower half). They show that the system switches to Receiver A in-service, and that this data burst occurred 10,000 error-free sync periods following the last error burst (approximately 7 s previous). The first error in the burst came 17,000 bit-times after the last sync pulse. The burst itself contained 11 errors in a burst length of 23 bits. The third group in the series shows that another burst started after 23 error-free sync periods. This burst started with an error 27,000 bits after the last sync pulse; it contained 18 errors in a length of 34 bits. The fourth group of octal words also shows that another receiver switch to Receiver B was made. All of this activity took place within a 100 ms interval (between the 38th and 39th index). A further look at data block No. 4 in Figure 3 shows that more burst-error data were received between indices 39 and 40; a total of six 3-word entries that we have not decoded.

The above example has been presented only to convey a sense of the methods used in both collecting these data and analyzing their results and meaning. The ITS is currently in the process of developing the computer routines and programs that will automatically retrieve, decode, and display these results in accordance with the analysis summaries outlined earlier in this section. When this project is completed, a technical report in the NTIA series will be published.

6. PRELIMINARY RESULTS AND DISCUSSION

Three specific periods of data acquired during the experiment have been analyzed and they are presented in this section as preliminary results. The selected data will illustrate the performance measure, the correspondence of the propagation factors, and some special measurement results. The preliminary data analysis does not include any summary of the burst-error statistics.

The first two samples of data that were analyzed were taken from periods of time when the measured multipath in the transmission channel was considered to be both "typical" and "severe." These characteristics are based on the magnitude of the delayed components, and the dynamic behavior as observed in the PN Channel Probe Data. A fairly typical period during the experiment was seen on 7 August 1981. The transmission channel was characterized by a strong superrefractive layer with its base at an elevation between 335 and 396 m (1100 to 1300 ft) above mean sea level (msl). The layer produced atmospheric multipath with delays on the order of 6 to 8 ns, where the delayed component was occasionally greater in magnitude than the more direct response. The multipath was observed in both diversity receive

channels, but generally not at the same time. A detailed description of the impulse response data (multipath) that are found to be quite typical for the PMTC test link can be found in the report by Hubbard (1979). Examples of the meteorological data (refractive index profiles) are given later in this section.

The type of multipath propagation that is created by the refractive layer over this path can be visualized from Figure 4. The figure is a ray-trace cross section¹ produced in a computer program, where the refractive index profile (computed from radiosonde data) is used to represent the propagation medium. In this case, the profile is shown as the modified refractivity in M-units (Bean and Dutton, 1966). One terminal of the LP-SNI link is indicated on the elevation ordinate. The outer terminal is shown at a distance of approximately 56.5 nmi (104 km). The multipath environment at the latter terminal is quite obvious from this figure. Other methods for relating the meteorological data and the measured multipath delays have been shown by Hubbard (1979; 1982). We include Figure 4 as one example of the ray-trace method. Examples of a graphical method are presented below.

Figure 4 illustrates that under the refractive conditions for the tests on 7 August 1981, the primary multipath is a result of surface reflection. This condition is created, however, by the elevated layer. This fact is confirmed from the ray-trace result shown in Figure 5. Here, a standard-atmosphere profile is used to characterize the propagation, and there is no resulting surface or other multipath from within the main lobe of the antenna patterns.

The data that have been analyzed for 7 August 1981 are summarized in Tables 4 and 5. At this time, both the PMTC radio and the DRAMA radio were under test over the same space-diversity link configuration. The performance data for each radio is therefore shown in the tables, and a direct comparison of their performance can be made. However, several important aspects must be considered before any quantitative conclusions are drawn on the basis of these data. These are:

1. The PMTC radio operates with a form of adaptive equalization in each receiver, which compensates for certain multipath distortions in the baseband signal (Hartman and Allen, 1979). The DRAMA radio did not use any form of adaptive equalization.
2. The two radio systems were operating over precisely the same space-diversity paths, but at different radio frequencies. Multipath propagation does not necessarily manifest itself on different

¹Courtesy of the PMTC Geophysics Laboratory (by permission).

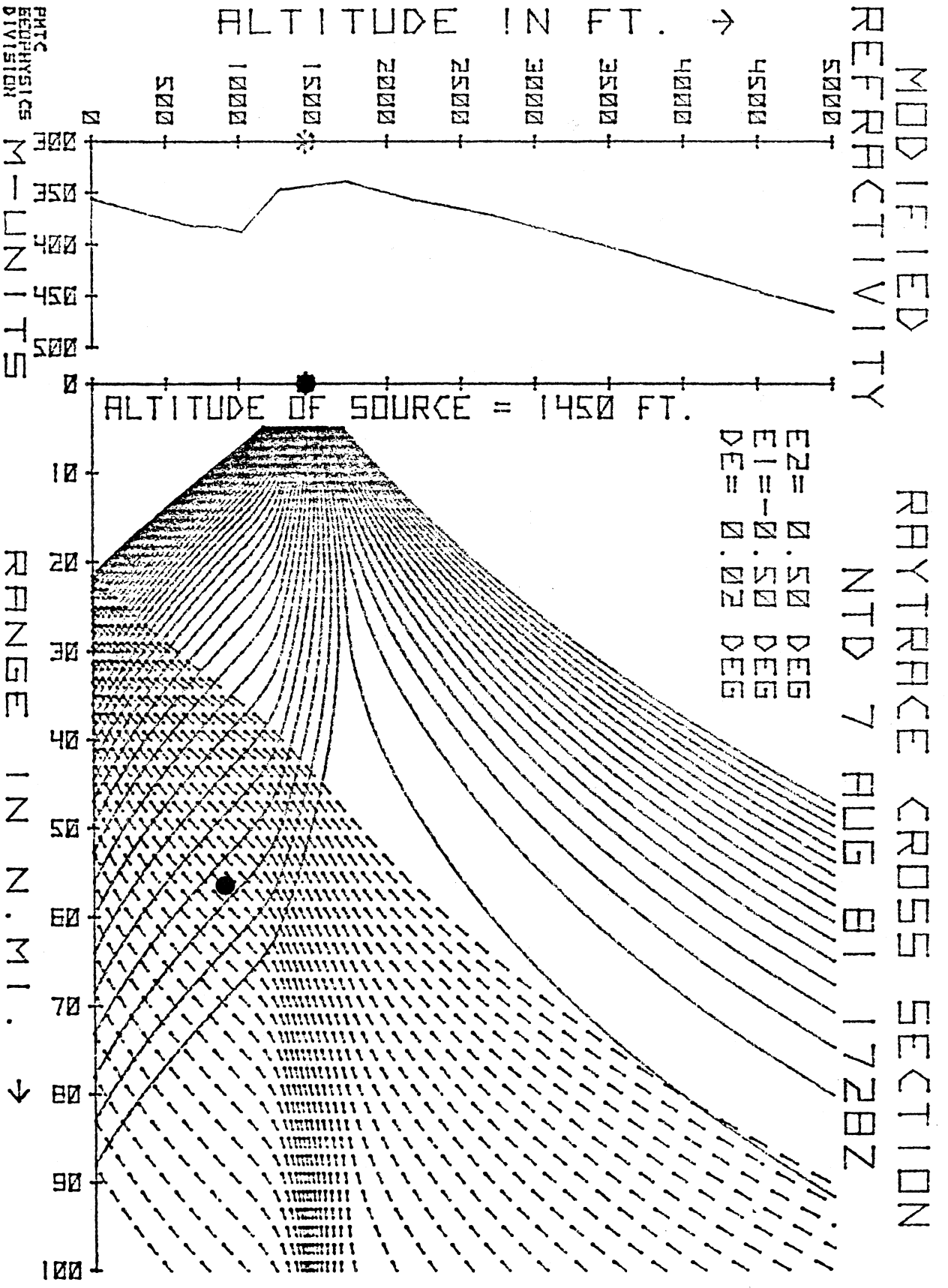


Figure 4. The modified refractivity profile and resultant ray-trace cross section for the LP-SNI link on 7 August 1981.

Table 4. Comparative Performance Data for 7 August 1981
(15-minute intervals)

Time (Z)	DRAMA Radio			PMTC Radio			Time Availability %	
	Err- Sec	Total Errors	BER	Err- Sec	Total Errors	BER	DRAMA	PMTC
0015	196	>	$>10^{-3}$	13	98,831,664	2.5(-3)	78.222	98.556
0030	182	>	"	2	157,147	4.0(-6)	79.778	99.778
0045	142	>	"	14	76,766,230	2.0(-3)	84.222	98.444
0100	261	>	"	8	28,204,802	7.0(-4)	71.000	99.111
0115	129	>	"	7	10,781,173	2.7(-4)	85.667	99.222
0130	266	>	"	7	427,749	1.0(-5)	70.444	99.222
0145	78	>	"	9	171,864	4.3(-6)	91.333	99.000
0200	153	>	"	19	18,494,451	4.6(-4)	83.000	97.889

>means counter overflow ($>10^7$)

Table 5. Comparative Performance Data for 7 August 1981
(1-minute intervals)

Time (Z)	DRAMA Radio			PMTC Radio			Time Availability %	
	Err- Sec	Total Errors	BER	Err- Sec	Total Errors	BER	DRAMA	PMTC
0210	6	38,045	4.9(-5)	0	0	0	90	100
0211	1	42	5.0(-8)	2	17,213	6.4(-6)	98.3	96.7
0212	16	416,546	5.4(-4)	0	0	0	73.3	100
0213	14	4,316,546	5.6(-3)	1	137	5.0(-8)	76.7	98.3
0214	11	309,707	4.0(-4)	0	0	0	81.7	100
0215	2	12	2.0(-8)	1	12	4.5(-9)	96.7	98.3
0216	6	12,802	1.7(-5)	1	40	1.5(-8)	90.0	98.3
0217	0	0	0	0	0	0	100	100
0218	12	4,752,229	6.1(-3)	0	0	0	80.0	100
0219	10	4,086,668	5.3(-3)	0	0	0	83.3	100
0220	12	169,050	2.2(-4)	0	0	0	80.0	100
0221	20	4,798,447	6.2(-3)	2	1,333	5.0(-7)	66.7	96.7
0223	10	---		0	0	0	83.3	100
0224	33	---		0	0	0	45.0	100
0225	11	1,180,729	1.5(-3)	0	0	0	81.7	100
0226	2	4	5.0(-9)	0	0	0	96.7	100
0227	2	6,925	9.0(-6)	7	4,638,705	1.7(-3)	96.7	88.3
Tots.	178	$> 20 \times 10^6$		16	4,657,440		Ave. 83.5	98.5

carrier frequencies at the same instants of time. Statistically, one might expect this disparity to vanish over a sufficient length of time. However, the data sample in Table 4 is not deemed to be long enough for such a conclusion. (This aspect will be treated in future analyses.)

3. The two radios both use diversity switching from one receiver to the other. However, the algorithms used for switching decisions are quite different (discussed later in this section).
4. The two radio systems operate with different modulation methods and mission bit rates. The PMTC mission bit rate was 44.7 Mb/s. The DRAMA radio was operated in a QPR mode with an aggregate bit rate of 26.112 Mb/s (composed of two mission bit streams of 12.928 Mb/s each). The spectra of the mission signal of the two systems are however, comparable. The bandwidths are approximately 20 MHz and 14 MHz, respectively.

The results in Table 4 show that neither of the two digital radios performed well in the multipath environment. In each 15 min. interval, the total bit-error count in the DRAMA radio data exceeded the allotted counter capacity (10^7 bits), so these results were lost. Over the entire 2-hour sample, the DRAMA radio registered nearly 18 times more errored-seconds than did the PMTC system. This factor is roughly the same when the data are compared on the basis of total errored-seconds, or on the average of the 15-min. interval data. A significant portion of this difference in performance can probably be attributed to the adaptive equalizer compensation in the PMTC radio. However, the other factors noted above may also be contributors to this rather disparate result.

The time availability factors given in Tables 4 and 5 are calculated as the ratio of error-free seconds to the number of seconds in the interval. These values indicate that the PMTC system performance was significantly better overall. However, the BER performance of this radio was much lower than desired.

Following the two-hour test shown in Table 4, a single 15-min. interval was analyzed where the data were accumulated in 1-min. intervals. These results are shown in Table 5. The errored-second data for each radio shows that this interval is very close to the median of the 15-min. intervals in Table 4. The DRAMA radio registered an excess of 20×10^6 bit-errors in the interval, which is equivalent to a BER of approximately 1.7×10^{-3} . The overall BER for the PMTC radio is on the order of 1.2×10^{-4} ; only about one order of magnitude better. However, it can be seen that the short-term (within the minute) data are considerably different. The last entry (0227Z) for the PMTC radio obviously has the greatest impact on the BER for the interval, as it consists of about 99.5% of all the errors made. If

this minute of data were dropped from the summary, the PMTC radio BER for the interval becomes 4.7×10^{-7} .

If a criterion for system outages is based on minutes in which the $BER > 10^{-6}$, the short interval of data in Table 5 would show that:

1. The DRAMA radio was below the performance threshold for 13 minutes; approximately 87% of the time.
2. The PMTC radio was below the threshold for 2 (non-consecutive) minutes; approximately 13% of the time.

Another way of measuring or comparing performance is based on the error-free seconds, which has been done in Tables 4 and 5 and listed as time availability (TA). On this basis, the difference in performance is not quite as extreme as those based on BER or BER/threshold, but it is still a considerable difference. These various measures of performance illustrate a problem that deserves greater attention. The measure used should be one that is most reflective of the performance or mission requirements of the system. For the tests reported here, the most meaningful data are considered to be the error-free seconds performance measure, with a detailed analyses (to be performed) that will characterize the distribution of errors within an errored-second and the distribution of the errored-seconds.

The performance data and the propagation data for the period 18-20 August 1981 was of particular interest. During this time, two 24-hour periods were observed that could be described as being among the best and worst performance periods. An interesting sidelight is that the two periods were contiguous. The performance data for each of these periods are presented in Table 6.

The first 24-hour run shows results that are near the desired performance for the PMTC radio (99.999% TA). However, in this period of mild multipath, the DRAMA radio performed below the desired or expected level. The errored-seconds are seen to be about 250 times higher, and the BER is worse by 4 orders of magnitude. The loss-of-sync data differ by a factor of 30.

The second 24-hour run (19-20 Aug.) represents a typically severe period of multipath activity. Here, the errored-seconds differ by a factor of approximately 5, and the BER performance factors are nearly the same for the two radios. However, the TA factor for the DRAMA radio has decreased by about 15 percentage points compared to less than 3 for the PMTC radio. Other status/alarm data may be compared from the entries in Table 6. Note, however, that some of these data are for individual receivers in the PMTC radio. The loss-of-frame sync and the BER alarm data for the DRAMA radio are for both receivers combined. The relative performance factor for this run (based on TA) is seen to be 1.15, which is close to that

Table 6. PMTC Radio Performance Data
18-20 August 1981

PERFORMANCE PARAMETER	TIME					
	2000Z 18 Aug (1300 PDT)	to	2000Z 19 Aug (1300 PDT)	2000Z 19 Aug (1300 PDT)	to	2000Z 20 Aug (1300 PDT)
PMTC Radio						
No. Errored-Seconds		2			2,311	
Total Bit Errors		34,581			> 10 ⁹	
Average BER		9.1x10 ⁻⁹			6.2x10 ⁻⁴	
BER > 10 ⁻⁷ (Rec. A)		127			9,450	
BER > 10 ⁻⁷ (Rec. B)		63			11,811	
Loss of Frame (Rec. A)		2			5,484	
Loss of Frame (Rec. B)		22			6,195	
Diversity Signal Loss		0			0	
Diversity Frame Loss		0			1,232	
Diversity Sync Loss		0			1,245	
% Error-Free Sec. (TA)		99.9976			97.3252	

DRAMA Radio

No. Errored-Seconds	497	10,147	**
Total Bit Errors	47,525,214	399,761,740	
Average BER	4.3x10 ⁻⁵	4.6x10 ⁻⁴	
No. Rec. Switches	1,056	13,125	
Loss of Frame Sync	697	29,719	
BER 10 ⁻³ (Alarm)	8,319	540,772	
% Error-Free Sec. (TA)	99.4248	84.7643	

** Based on 18.5 hours of data; 5.5 hours lost when data system ran out of tape.

calculated for other test periods. The loss of data for the DRAMA radio would have an effect on this result.

In the following paragraphs, we will discuss the results shown in Table 6 with respect to the propagation and meteorological data.

The refractivity structures in the atmosphere for the dates 18 and 19 August were obtained from the PMTC radiosonde data. We include plots of these profiles as examples to convey the source of the atmospheric multipath, and essentially to close the loop on the related analyses used in the data processing; i.e., the radio performance data, the propagation (impulse response) data, and finally the meteorological data.

The refractivity data were measured and furnished to ITS by the PMTC Geophysics Laboratory. This group obtains at least two soundings of the atmosphere each day; one taken on the coast at Point Mugu and a second sounding from SNI. These data have proven to be invaluable in analyzing the source of multipath over the LP-SNI link. The techniques that have been used are reported by Hubbard (1979). Specific examples of these analyses are presented later in this section.

Figures 6 and 7 show the refractivity structure measured on 18 August 1981. Figure 6 shows the profiles as they appeared near LP (Point Mugu data), and Figure 7 shows the companion soundings made at SNI. Note that a very strong inversion/ducting layer is seen in both sets of profiles, and that it was very stable in elevation for a period of several hours between soundings. Several other features should be noted:

1. The gradient of the layer is extremely superrefractive; well above a trapping value.
2. The layer is tilted downward off the LP coastline, as its elevation is approximately 150 m (500 ft) lower at SNI during the soundings of late afternoon and evening.
3. The layer is well above the normal propagation path, as can be seen from its height with respect to the LP and SNI terminal elevations shown on the ordinates of the figures.

In the references noted previously, it has been shown that this refractive condition on the LP-SNI link produces multipath delays that correspond geometrically with the boundaries of the layer. When the refractive layer is as high above the path as it is in this case, the layer is not well illuminated by the link antennas. Thus, the multipath components are typically long in delay but low in magnitude. This is consistent with the data measured in the experiment on this date. However, when the refractive layer is tilted in elevation, the possibility of significant multipath is increased.

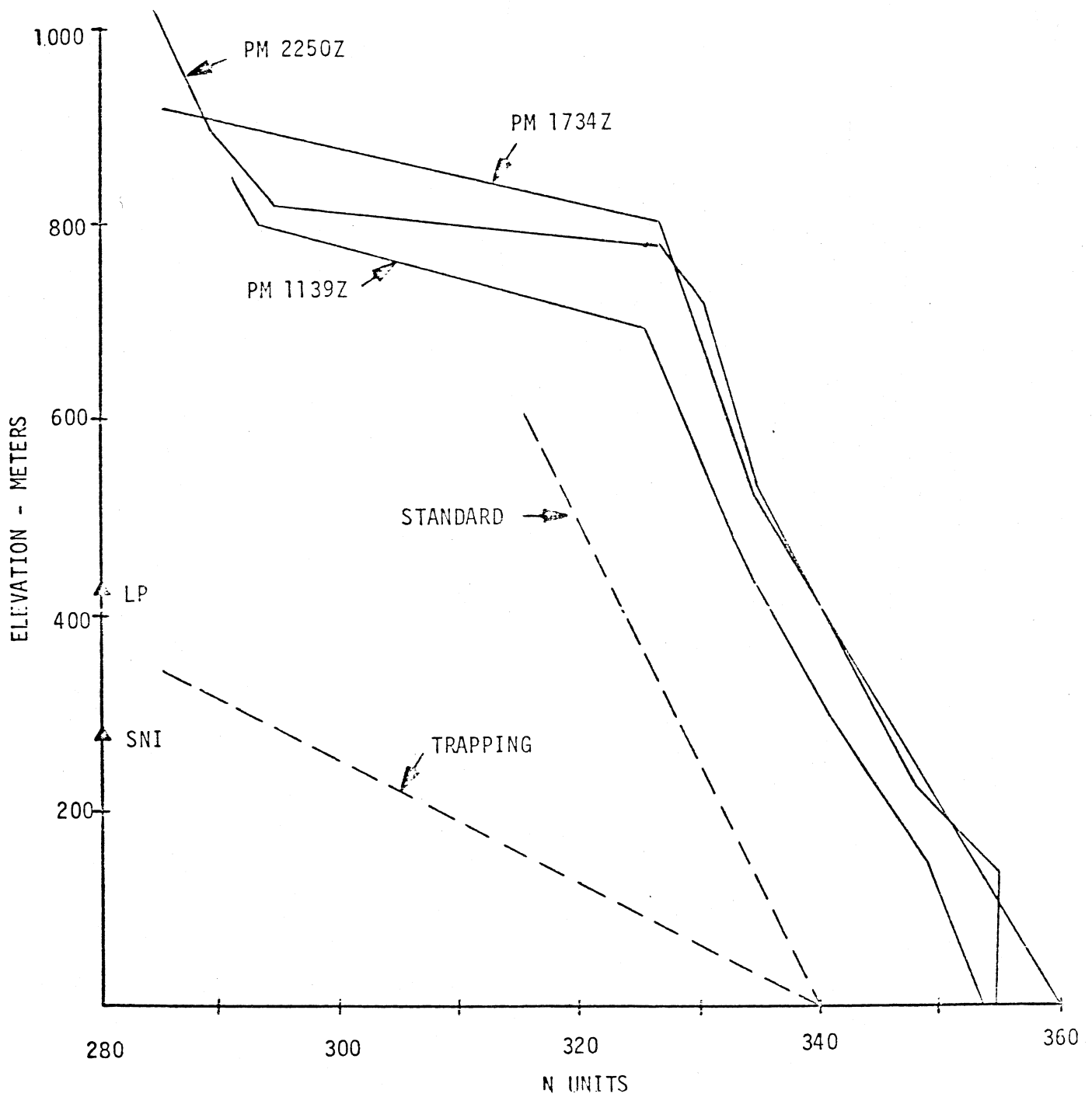


Figure 6. Refractive index profiles measured at Point Mugu on 18 August 1981.

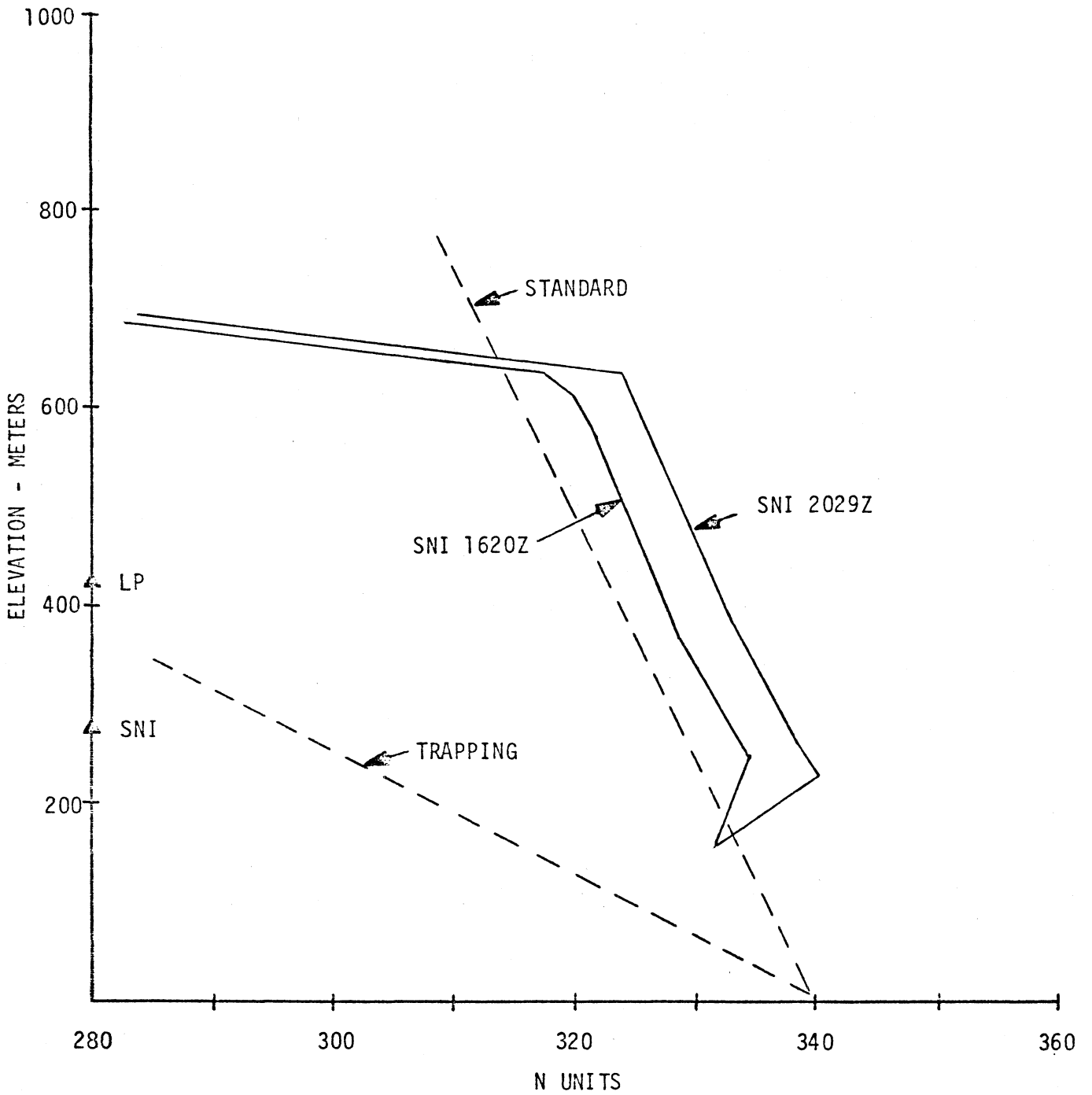


Figure 7. Refractive index profiles measured at San Nicolas Island (SNI) on 18 August 1981.

The performance of both radios began to degrade very noticeably between 1800Z and 2200Z on 19 August, and the poor performance lasted until around 0700Z on 20 August. The refractive profiles measured on 19 August are shown in Figure 8, which includes both the Point Mugu and SNI soundings. There was no sounding from SNI during the early hours of the day, but the early sounding from Point Mugu indicates that the layer was quite high in elevation. The 1732Z sounding from PM shows that the layer had lowered to around 732 m (2400 ft) at that time, some 122 m (400 ft) lower than the 1138Z sounding. Both the PM and SNI data taken around 2200Z on this date, show that the layer had become lower yet in elevation by 304 m (1000 ft) more. The most significant features at this time are that the base of the layer is seen to be below the elevation of the terminals, and the layer is again tilted downward toward the SNI terminal. The time of these soundings corresponds very closely with the change observed in the radio performance data. Geometric delay-spread correspondence has been established in the following discussion, and there can be little doubt that the refractive layers cause the strong multipath. This was illustrated earlier in the ray-tracing results of Figure 4.

Ray-tracing analyses generally cannot convey the complete propagation picture, because of the restrictions on the meteorological data that can be used in the computer program. For example, most programs can only make use of one refractive profile. Thus, it must be assumed that the structure is uniform along the entire path. This is frequently not the case, as seen by the tilted layers measured in the PMTC data. Also, small variations in the refractive profile are often impossible to include, and only a straight line segmented approximation to the measured profile can be used. The methods are valuable however in establishing the possibilities for the origin of multipath signals.

The second method for evaluating multipath and meteorological data has been referenced previously. It is based on a geometric approach, using reflective analysis techniques. It is conceded that multipath from atmospheric layers is most probably due to refraction (the assumption made in ray tracing) rather than reflection. However, it has been found that if one applies the reflective geometry to either atmospheric or surface generated multipath, there is usually a good correspondence with measured delay-spread values. The method involves calculating and plotting the elliptical locus of delay values (taken from measured impulse response data) on the profile of the propagation path. The latter is plotted with respect to the appropriate k-factors, calculated from the segmented features of the refractive data. Examples of this analysis are presented below that are relevant for the data of Table 6.

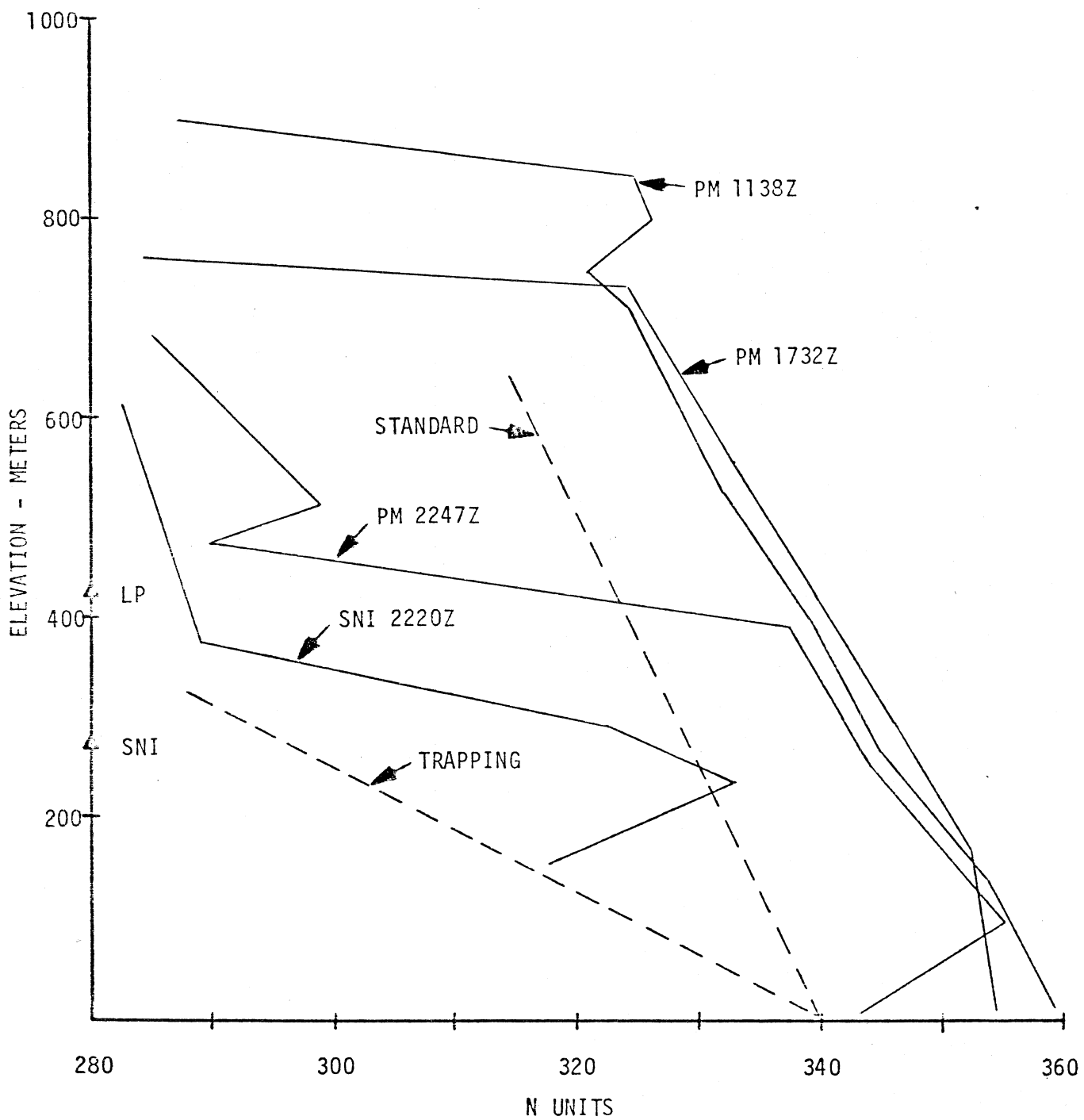


Figure 8. Refractive index profiles measured at Point Mugu (PM) and San Nicolas Island (SNI) on 19 August 1981.

For these examples we use the multipath data measured at PMTC on 18-19 August 1981, where the time delays were on the order of 5 and 14 ns. These values were measured over a period of approximately 4 hours between 2200-0230Z (1500-1930 PDT). The corresponding radiosonde data for this period are given in Figures 6 and 7; the PM 2250Z profile and SNI 2029Z profile, respectively. These profiles show that a very strong refractive layer was persistent over the path, slightly lower in elevation at the SNI terminal. Below the layer, and down to an elevation lower than that of the two radio terminals, the refractivity gradient is near a standard value ($k=4/3$). Note however, that both refractive profiles show that a subrefractive condition (slopes more positive than standard) was measured nearer the surface. The SNI sounding did not contain data lower than that plotted, so the subrefractive region is not traceable all the way to the surface. The subrefractive condition is important, as it can explain the origin of some of the measured multipath.

Figure 9 has been plotted to illustrate the above conditions. The superrefractive layer is shown in the shaded area, plotted on the basis of a $4/3$ (standard refractivity) earth radius. This k -factor also applies to the solid line plot of the surface profile. The radio terminals are seen to be within the standard refractivity region. Thus, the direct-path radio rays are plotted as straight lines between the terminals. For the measured delay-spread values of 5 and 14 ns, two locii (half-ellipse for each) have been plotted on the figure. These Fresnel ellipsoids define the locus of all points from which multipath signals could emanate with the given delay value, if the signals were reflected. Note that the 14 ns ellipse is tangential to the refractive layer, and clearly indicates that this is the source of the measured multipath with that delay value.

The source of the shorter 5 ns delay is not, however, as well defined. We note that this ellipse does not correspond to any meteorological feature, and it is not tangential to the $4/3$ earth profile. However, the subrefractive gradients at the lower elevation in the radiosonde data become important in this case. The PM sounding shows a near-zero gradient, and the SNI sounding shows a significant, positive gradient. These gradients will definitely affect the propagation near the earth's surface.

One method of analyzing the subrefractive region in the graphical form is included in Figure 9. First, the boundary between the $k=4/3$ region and the subrefractive region has been sketched near the elevation of 200 meters. The approximate level of the boundary is taken from the two profile curves of the

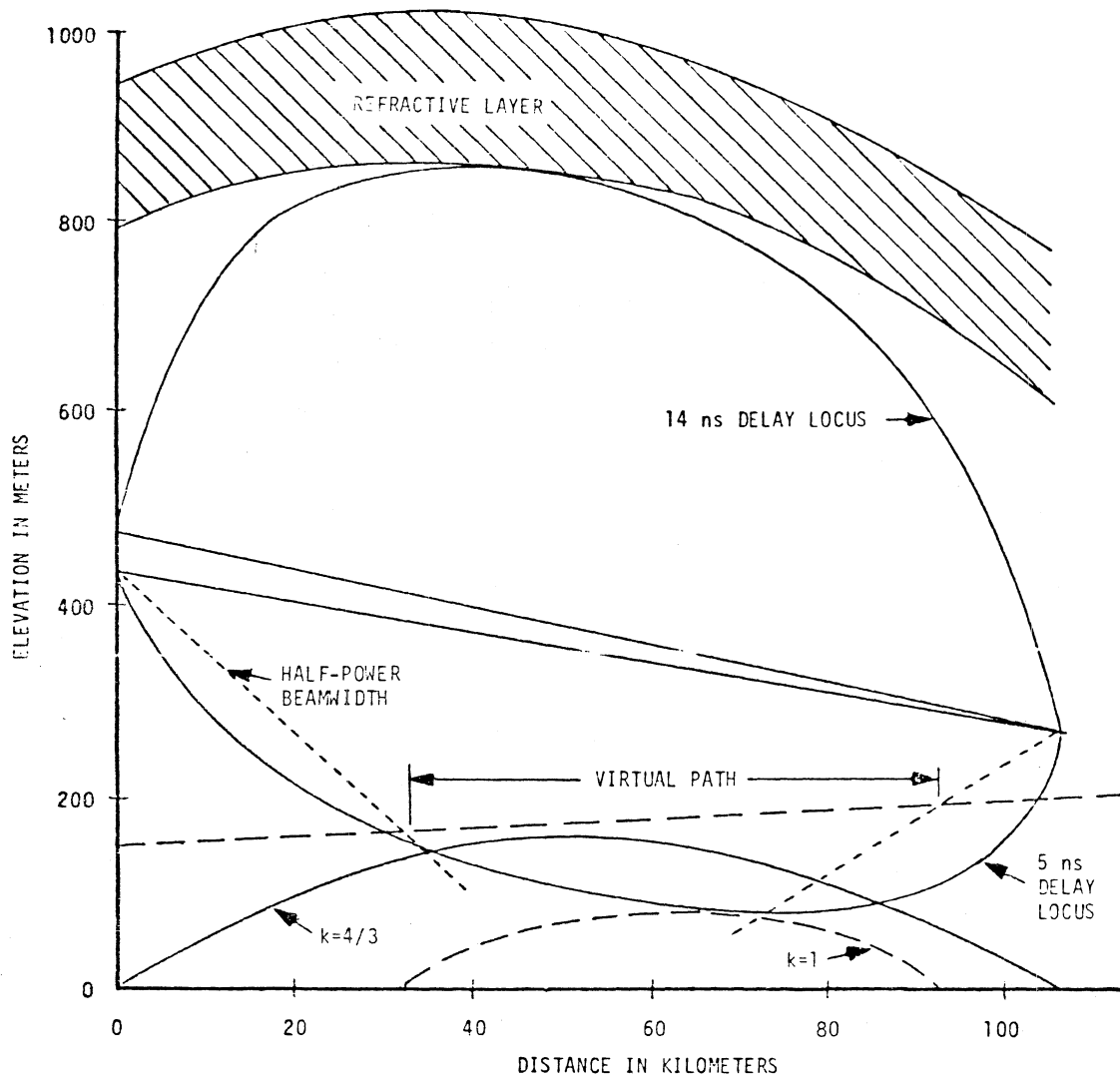


Figure 9. Graphical correspondence between delay-spread measurements and the refractivity data on the LP-SNI link on 18 August 1981.

radiosonde data. Second, we sketch the half-power beamwidths of the antenna system (lower bounds) within the 4/3 earth region of the figure. The intersection of these lines with the boundary line for the subrefractive region essentially defines a new propagation path. For example, radio rays from the terminals would follow straight line paths (within the half-power beamwidth for significant rays). At the intersection between the 4/3 earth geometry and the lower region with subrefractivity, the rays would curve through the lower atmosphere before rising again to the antennas. At these points of intersection, we can consider a secondary propagation path with hypothetical radiators at the intersection points. The new path would exist only within the subrefractive region, and a new effective surface profile may be computed. Note that the hypothetical path is roughly half the length of the true path, and for this reason the effective earth profile will be considerably lower for the subrefractive condition. The modified earth-surface profile for the subrefractive path is shown in Figure 9 by the dashed-line curve. This is only an estimate since the subrefractive gradient in the two refractive profiles is not well defined by the measurements. We note from Figure 6 that the gradient near the surface at PM (2250Z) is just slightly positive. The SNI gradient from Figure 7 is much more positive. In the range of positive gradients, the k-factor does not change rapidly with gradient. For example, a gradient range from 0 N/km to +157 N/km has a k-factor range of only 1.0 to 0.5, respectively.

The modified earth profile in Figure 9 was calculated for a $k=1$ value. The most important result is that a good tangential relationship is seen between the 5 ns delay locus and the modified profile. This very strongly indicates that the shorter delay multipath is a result of surface reflection, and it is longer in delay than would be expected from a standard refractive gradient.

We have previously noted that the refractive layer on 19-20 August moved to a lower elevation late in the day. This is seen from the refractivity profiles shown in Figure 8. The delay-spread for this period of time was approximately 16 ns. It was also at this time that the radio performance began to degrade seriously. The refractivity data indicate that both radio terminals were within a ducting layer, and the gradient within the layer was on the order of -800 N/km. Thus, in this case we can assume that the radio rays for the most direct path are trapped within the layer, and the mechanism is ducting. Below the layer the refractivity is mixed. The PM sounding shows near-standard conditions down to an elevation of about 100 m. The SNI sounding shows a positive gradient beginning at the lower boundary of the layer.

Figure 10 presents the graphical analysis of the multipath for the above conditions. Here the effective earth profile for the multipath becomes concave with respect to the ducting layer and the ray path, as we have assumed trapping for the direct path signal. The predominant delay time of 16 ns was used to calculate the ellipse shown. In the analysis we have followed the same procedures as those outlined above. The boundary of the subrefractive region has been shown with the dashed line. The virtual path within this region is approximately 70 km in length, and the refractive gradient is on the order of 180 N/km in both profiles (Figure 8). Using these values for the virtual path, and standard refractivity for the 35 km from LP, the effective earth profile is modified in the boundary region. A good agreement is found between the modified earth profile and the delay ellipsoid. Thus, the longer delay component, which was seen to be quite strong in magnitude, is apparently from a surface reflection. We present these examples to illustrate the correspondence between the meteorological data and the propagation measurements.

The final data that were analyzed for this preliminary summary were taken from a set of special tests that were conducted on the last two days of testing (1-2 September 1981). As was noted previously, the strong elevated superrefractive layer that was observed during the latter part of August persisted through the remainder of the test period. The gradient of the layer was fairly constant, and only its elevation changed significantly with time. These features are shown in the refractivity profiles of Figure 11. The superrefractive layer in each of these profiles has a gradient on the order of -820N/km (-250N/kft); this together with the near-standard atmosphere immediately below constitute an elevated duct [Dougherty and Dutton, 1981]. Radio rays that strike this layer are bent back toward the earth's surface. This is shown in the ray-trace diagram of Figure 12, and from this diagram it can be seen that the multipath is completely developed from the elevated atmospheric duct. In general, the multipath delay becomes shorter as the layer moves down in elevation.

The objective of the special test series was to obtain some comparative performance data from the two radio systems, operating in both a diversity and a non-diversity mode. Added to this configuration change was the ability to turn the adaptive equalizer (AE) in the PMTC receivers on and off. It was anticipated that these changes in configuration would permit a comparison of the diversity performance between the two radios, and some quantitative measure of the improvement realized from the AE in the PMTC radio.

The first of the special test runs was conducted on 1 September 1981 for a period of several hours. During this period, the AE's in both receivers of the

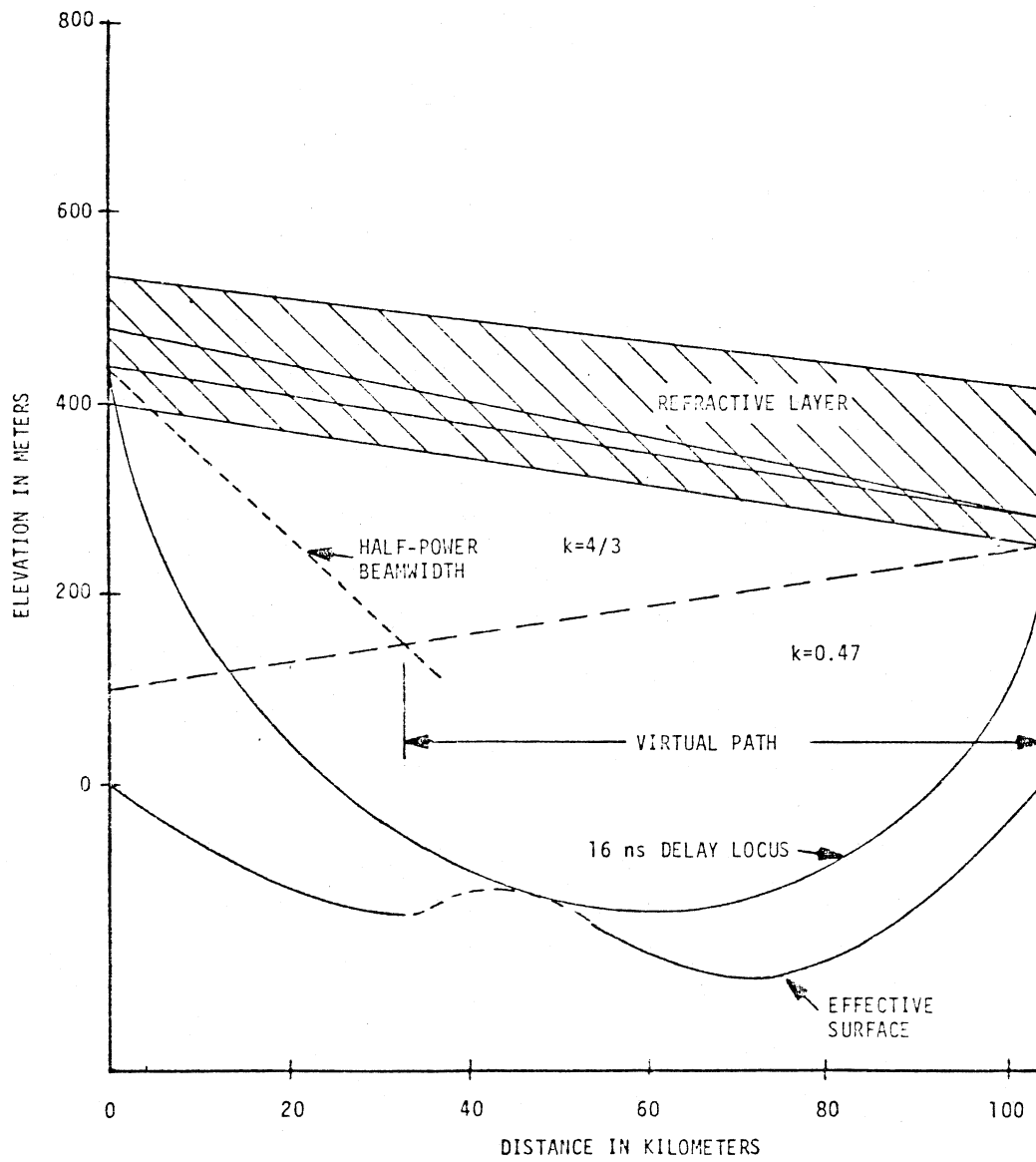


Figure 10. Graphical correspondence between delay-spread measurements and the refractivity data on the LP-SNI link on 19 August 1981.

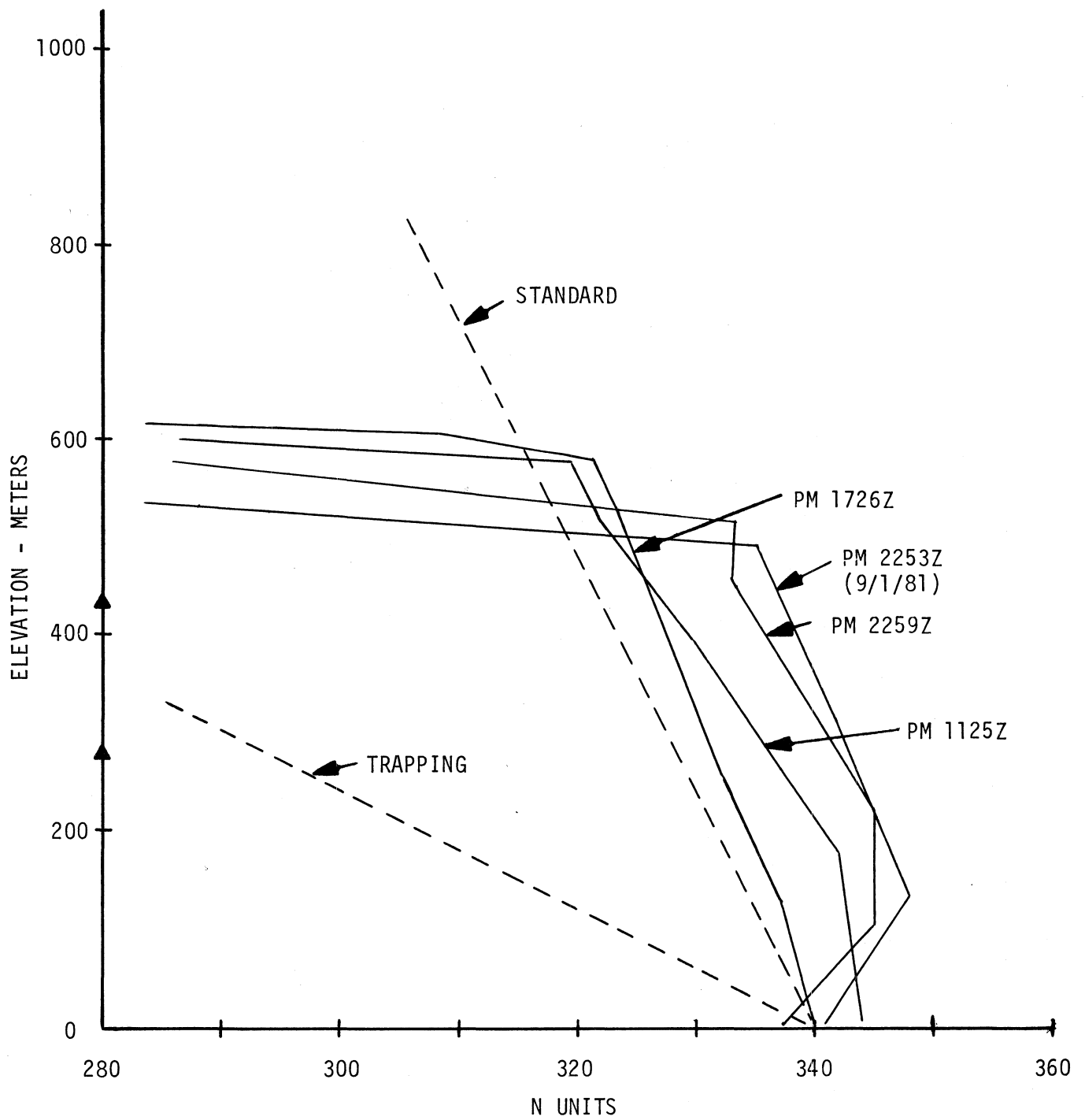


Figure 11. Refractive index profiles measured at Point Mugu (PM) on 1-2 September 1981.

MODIFIED
REFRACTIVITY

RAYTRACE CROSS SECTION
NTD 2 SEP 81 1726Z

42

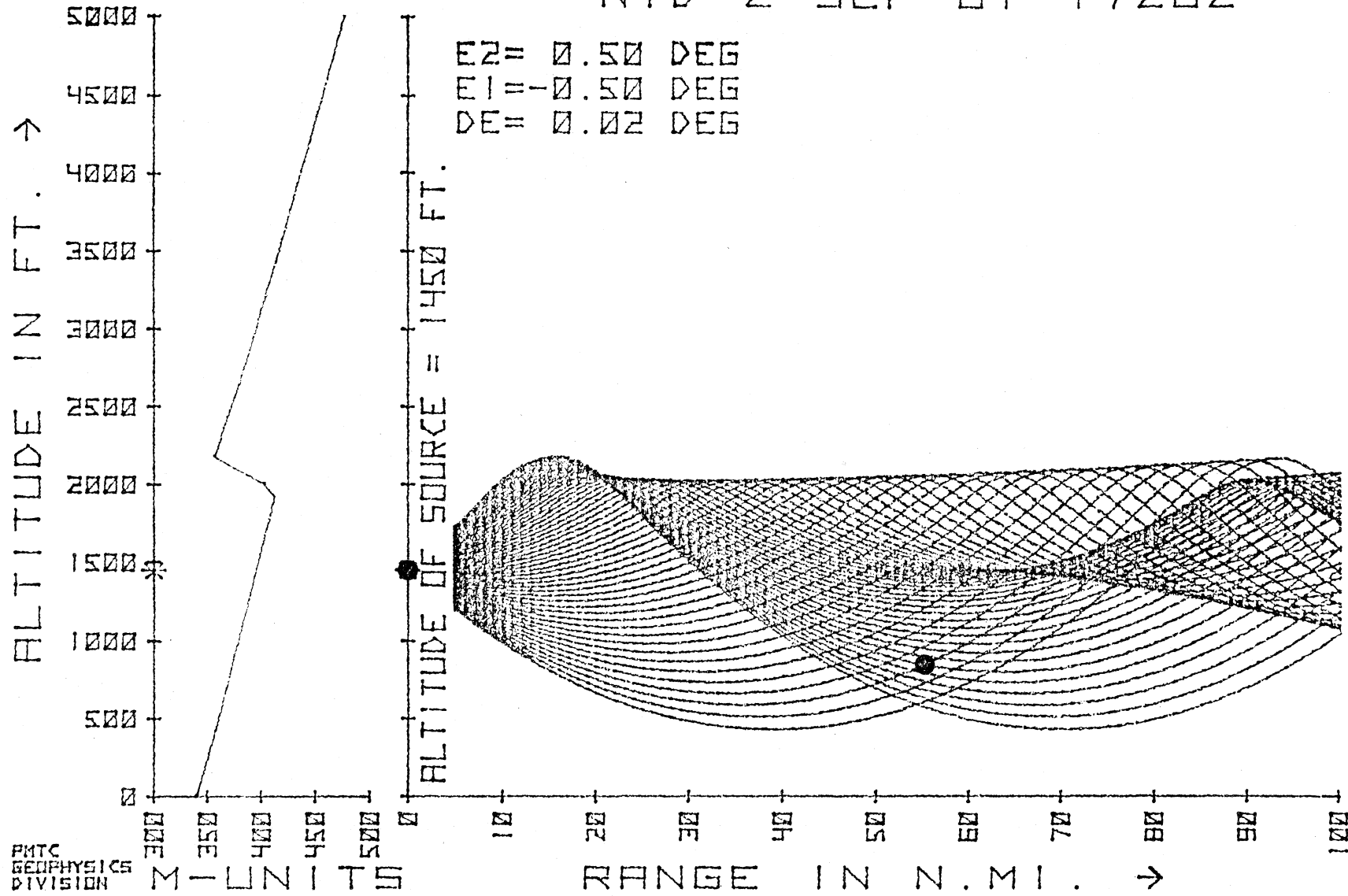


Figure 12. The modified refractivity profile and the resultant ray-trace cross section for the LP-SNI link on 2 September 1981.

PMTC radio were switched off, thus providing a measure of the basic space diversity performance only. One hour of these data has been analyzed on the basis of errored-seconds and total error performance. The results are presented in Table 7, where we have listed the data minute-by-minute over the hour. However, we have omitted those minutes in which neither radio registered any error data. It is clear from this tabulation that the PMTC radio performed much better than did the DRAMA radio. This result is somewhat surprising when the differences in modulation and mission bit rates are considered. Also, the multipath effects were more severe on the PMTC frequency, as will be seen in subsequent data.

Based on all of the errored-second data, the percent of error-free seconds (or time availability) is shown at the bottom of Table 7 for each radio system. We again see that the relative performance factor is on the order of 1.2 better for the PMTC radio, which is the same result found in the performance data summarized in Tables 4 and 5 for 7 August 1981. In addition, the BER performance over this hour is almost 2 orders of magnitude better for the PMTC radio.

If the TA factor is based on errored-seconds data in which a threshold of $BER > 10^{-6}$ is used (as marked in Table 7), the performance level for the PMTC radio is not changed. The factor for the DRAMA radio is improved from 84.6% to 87.1%, but both are well below the desired level.

The results of this test lead to a qualitative conclusion that the diversity switching algorithm in the PMTC radio is superior to that used in the DRAMA radio. The DRAMA system used a switching algorithm based on a comparison of the RSL in the diversity receivers, which selected the higher of the two. Earlier ITS investigations also suggested that RSL is not an adequate criterion on which to base diversity switching [Dougherty and Hartman, 1977]. The PMTC radio used an algorithm that is based on several performance factors. These included the RSL as well as a measure of the digital data performance from pseudo-eye pattern detectors. Other receiver-status alarms were also used. These factors were registered in a 20-bit digital word for each receiver, and the weighted evaluation of these two words was used to select the on-line receiver. Both systems used a data clock recovery scheme that preserved the bit-count integrity (BCI) where switching took place. It is beyond the scope of this report to present these operating features in any greater detail.

The data in Tables 4 and 5 were recorded with the AE's in the PMTC radio operating in both receivers. Since the relative performance factor in the earlier summary and that in Table 7 are nearly the same, it is not possible to detect an improvement factor for the AE's independently. Thus we conclude that the improvement from the AE's must be more subtle than the diversity improvement

Table 7. Radio Performance Data on 1 September 1981

Time (Z)	PMTC Radio			DRAMA Radio		
	Err-Sec	Errors	BER >10 ⁻⁶	Err-Sec	Errors	BER >10 ⁻⁶
2119	0	0		2	18	
2120	0	0		30	2,185	X
2123	0	0		12	38	
2125	0	0		8	21	
2129	0	0		29	7,500	X
2131	0	0		19	4,010	X
2133	0	0		19	157	
2135	0	0		6	54	
2137	13	14,120	X	11	199	
2138	0	0		9	38	
2140	0	0		16	1,898	X
2141	0	0		2	3	
2142	0	0		20	452	
2144	0	0		33	2,818	X
2145	0	0		1	2	
2146	0	0		19	1,079	X
2147	0	0		38	304,474	X
2148	0	0		25	11,953	X
2150	0	0		77	692,378	X
2153	0	0		39	14,074	X
2156	0	0		1	1	
2157	4	58,640	X	0	0	
2158	0	0		1	1	
2159	0	0		2	3	
2201	0	0		45	187,110	X
2202	0	0		10	70	
2208	0	0		9	61	
2209	0	0		4	10	
2211	0	0		57	1,652	X
2212	0	0		11	55	
2215	0	0		37	1,754	X

Totals: 17 72,760 2min 592 1,234,068 13min

BER Over the Hour:

PMTC Radio: 4.52×10^{-7}

DRAMA Radio: 2.65×10^{-5}

Time Availability:

PMTC Radio: 99.5%

DRAMA Radio: 84.6%

System Configuration Notes:

Space Diversity/Switched Combiners - Both Radios
Adaptive Equalizers in PMTC Radio Receivers were Switched OFF

factor, and a quantitative value must await the detailed analyses of the error-distribution data. It is conceivable, for example, that had the AE's been operating during the test in Table 7, they may have modified considerably the error count and distribution of errors in the two PMTC data entries.

In order to gain more insight into the results of the test summarized in Table 7, we have examined the multipath data for the period. An analysis of the impulse response showed that the multipath component was very strong and had a nominal delay of 4 ns during the test period. This value is consistent with the position of the refractive layer shown by the profile of 2253 Z on 1 September 1981 (Fig. 11). The result is based on the graphical approach illustrated by Figures 9 and 10.

Figure 13 is provided to illustrate the frequency selective fading that would result from the measured impulse data. The theoretical transfer function for a two-path transmission model is illustrated in the figure, where the multipath component has a magnitude of 0.9 times that of the direct path signal. The solid line plot represents the transfer function where the two components are in phase. The dashed line function is for an out-of-phase condition. The null-to-null spacing on the diagram is calculated from

$$\Delta f_n = 1/\tau = 1/4 \text{ ns} = .250 \text{ GHz},$$

where f_n is the frequency of a transfer function null, and τ is the delay time of the multipath component. The actual frequency at which the nulls fall is obviously a function of the phase between the component signals. For illustration purposes, we have arbitrarily positioned the nulls with respect to the operating frequency of the PMTC radio (7.35 GHz). The DRAMA radio was operated at a carrier frequency 790 MHz higher, at 8.14 GHz. Since the theoretical transfer function is repetitive, there is an effective frequency separation between the two carrier frequencies that can be found as follows. With $\Delta f_n = 250$ MHz, it can be shown that the DRAMA carrier frequency would fall on the diagram at a point 3.16 lobes ($790/250=3.16$) above the PMTC frequency. This position is completely equivalent to a position 0.16 lobes above the PMTC carrier or 40 MHz higher in frequency. Thus, the effective DRAMA radio carrier is shown at this relative position in Figure 13. In addition to the two carrier positions, we have sketched the relative signal bandwidths for both radios in the figure.

The significance of the illustration is to note that if the multipath is causing only slope distortion in the spectra of either radio, the other is operating near a peak of the transfer function, and very little multipath distortion would be expected. A physical example of this fact is shown by the spectral data plotted

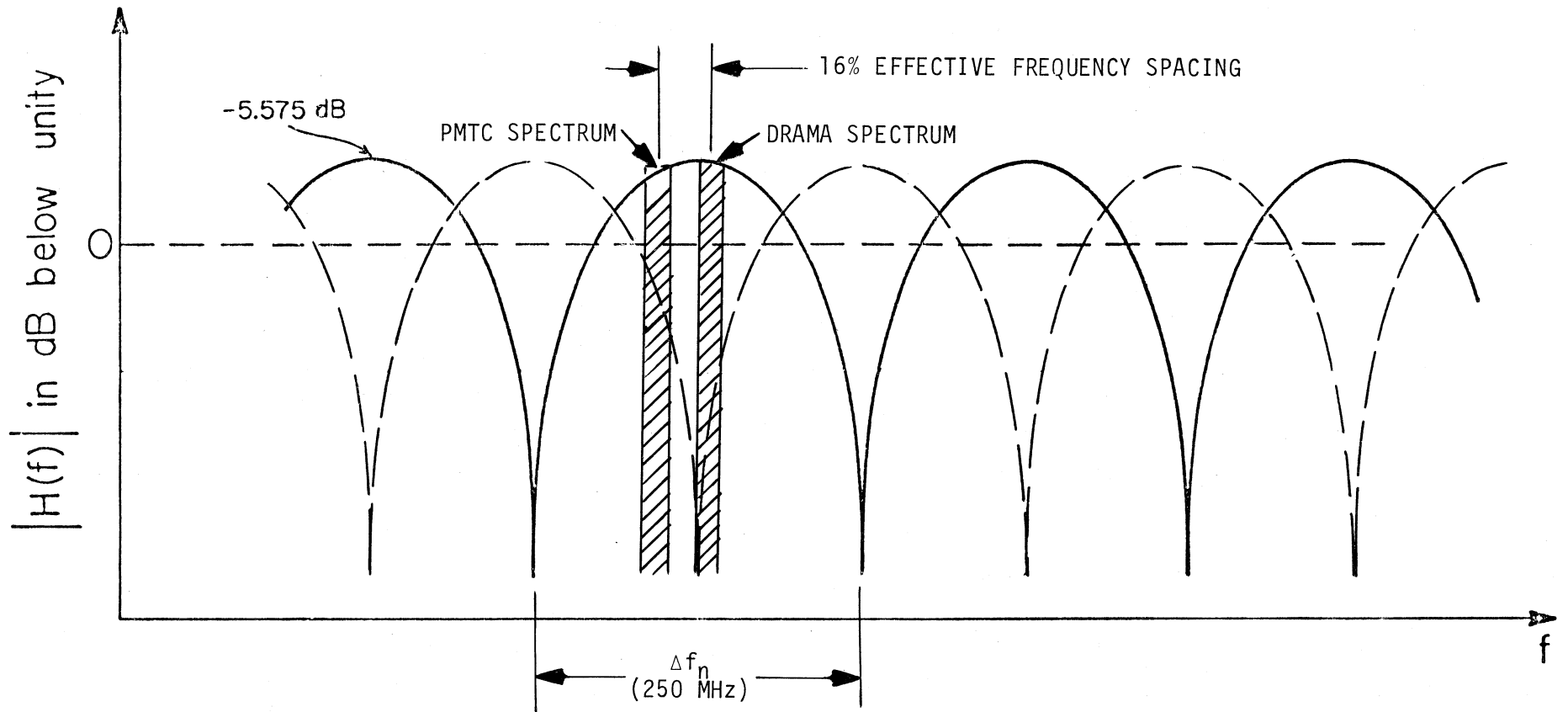


Figure 13. The theoretical frequency transfer function of the transmission channel for the multipath conditions on 1 September 1981. The illustration applies to the nominal multipath delay of 4 ns, measured during the interval of the data presented in Table 7.

in Figure 14. Here, the signal spectra from each of the four receivers are displayed for a section of the measured data. Note from the individual data records that the functions are not all contiguous in time, but those within each 5 s record are. These data were recorded on the digital data tapes, and were played back in sequence through a graphics display. Each spectral function was measured in a 1-s interval, and 25 are displayed in the figure. The top function for each radio was measured from the lower diversity antenna, and the lower function from the upper diversity antenna.

The difference in the shape of the spectral functions for the two radios should be explained. Each radio uses a form of data scrambling at the transmitter to equalize (more or less) the spectral distribution of the transmitted data regardless of its content. The PMTC radio also develops a signal spectrum that is fairly uniform in density (flat) across the bandwidth. This characteristic is evident in the function for the upper-diversity PMTC signal in Figure 14. The spectra shown in the top display of Figure 14 are seen to be distorted on the low-frequency edge of each spectral plot. This tilt is typical of the multipath distortion, and the result is easily visualized from Figure 13. Without the "flat" spectral shaping, distortion in the DRAMA spectral functions are not as readily seen. However, very little distortion is seen in those plotted in Figure 14 -- consistent with the theoretical sketch of Figure 13. Also, there is little evidence of distortion in the spectra from the upper-diversity PMTC signal. Even though a strong multipath component was measured in both diversity channels, the relative phase (or delay) was obviously not the same in both channels. Figures 13 and 14 thus display an effect of both space and frequency diversity discrimination against multipath. The ideal frequency diversity for any given multipath component is easily determined. For example, if the effective carrier frequency spacing is one-half the value of Δf_n , this would assure that a transfer function null would affect only one frequency at a time. When a null coincides with one carrier, the other would fall at the peak of the transfer function. Unfortunately, in an atmospheric/dynamic channel, the delays do not remain constant. A pair of frequencies that are ideally separated for one delay value can lose all diversity advantage at a different delay. This occurs whenever the effective frequency spacing approaches either zero or the value of Δf_n .

It was anticipated that in performing tandem tests of diversity and non-diversity performance, a measure of the space diversity improvement factor for each radio might be derived. However, as will be seen from the results presented

1 September 1981
2147:01Z

PMTC SPECTRA

Low Antenna

High Antenna

DRAMA SPECTRA

Low Antenna

High Antenna

2147:06Z

2147:16Z

2147:21Z

2147:26Z

48

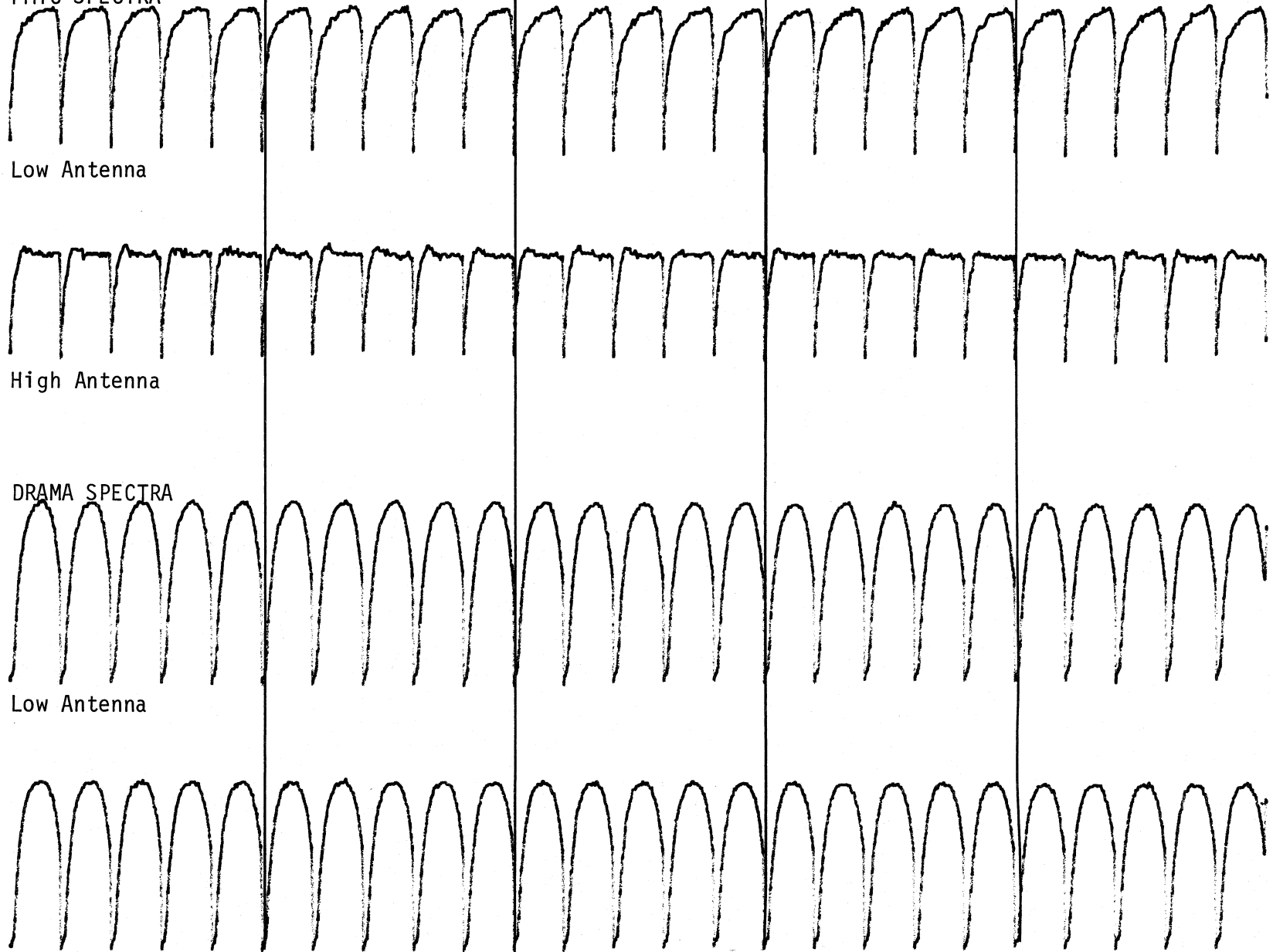


Figure 14. A sample of the received signal spectra measured from both radios during the interval of test data given in Table 7.

below, the multipath conditions changed too rapidly during the test period to permit a stable evaluation. The three nondiversity tests were performed on 2 September 1981. The results are shown in Figure 15, where the performance has been plotted in terms of the TA factor for all errored-seconds. The first test, conducted between 1730-1830 Z, was for reception from the lower diversity antenna on each radio, and the AE's in the PMTC radio were off. The multipath delay at this time was measured to be approximately 10 ns. This is equivalent to about a 90% effective frequency separation. Under these conditions we would expect the frequency nulls of the transfer function to effect both frequencies close together in time, as the relative phase or delay time changes. This result is evident in the spectral data shown in Figure 16. The figure shows 25 contiguous spectral functions, measured from the lower diversity-channel receiver in each radio system. A frequency selective "notch" is seen to have moved through both signal spectra during the 25 s interval. An interesting fact can be deduced from these data. It can be seen that the frequency selective notch has moved through the spectra in opposite directions in the two receivers. This implies that the channel dynamics must involve a change in both time delay and in relative phase. The effect can be visualized using Figure 13. A delay value that increases slightly (thereby decreasing the null-to-null spacing in the transfer function), or a change in relative phase at a fixed delay would independently cause a null to move through the spectra in the same direction.

Since the effective frequency spacing during this first test is quite large (90%), we can assume that the frequency diversity effects will be small, and thus draw some valid conclusion relative to the space diversity/nondiversity performance. The mean nondiversity performance levels during the first test in Figure 15 are as follows:

PMTC Radio : $\overline{TA} = 64.73\%$

DRAMA Radio: $\overline{TA} = 72.27\%$.

Comparing the above values with the space diversity values of Table 7, we compute the following:

Space Diversity Improvement Factor

PMTC Radio : 1.54

DRAMA Radio: 1.17.

These results may be questionable because of the uncertainty in tandem measurements, the assumption of low frequency diversity action, and the short duration of the test periods.

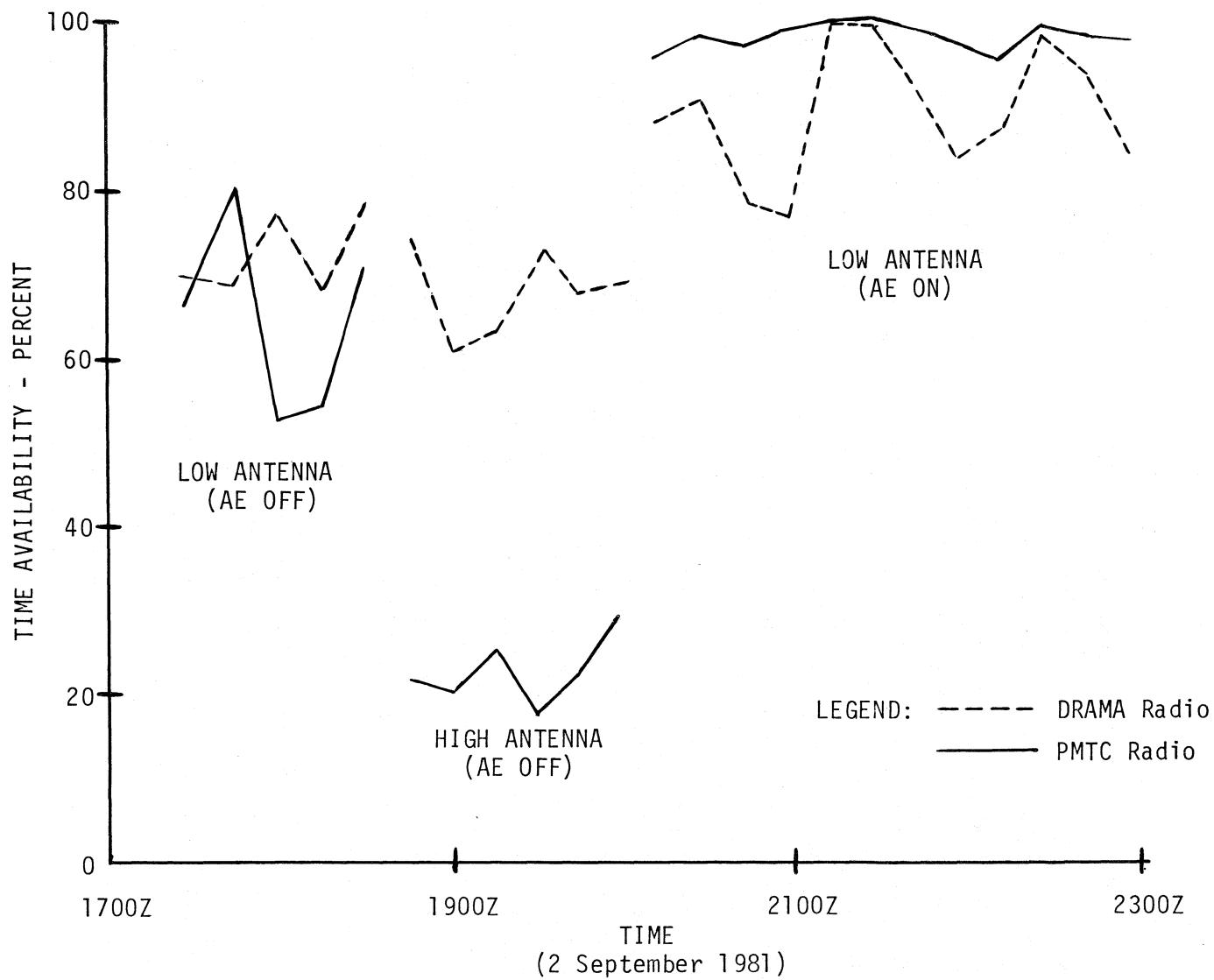
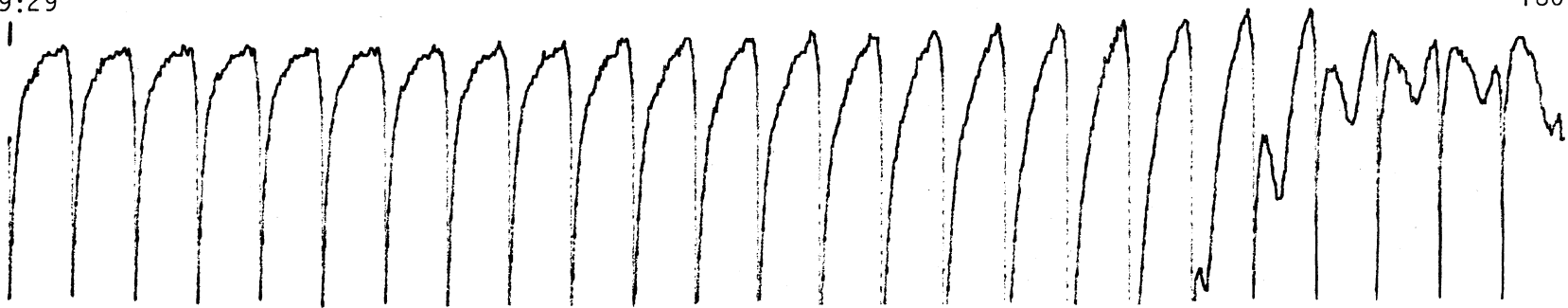


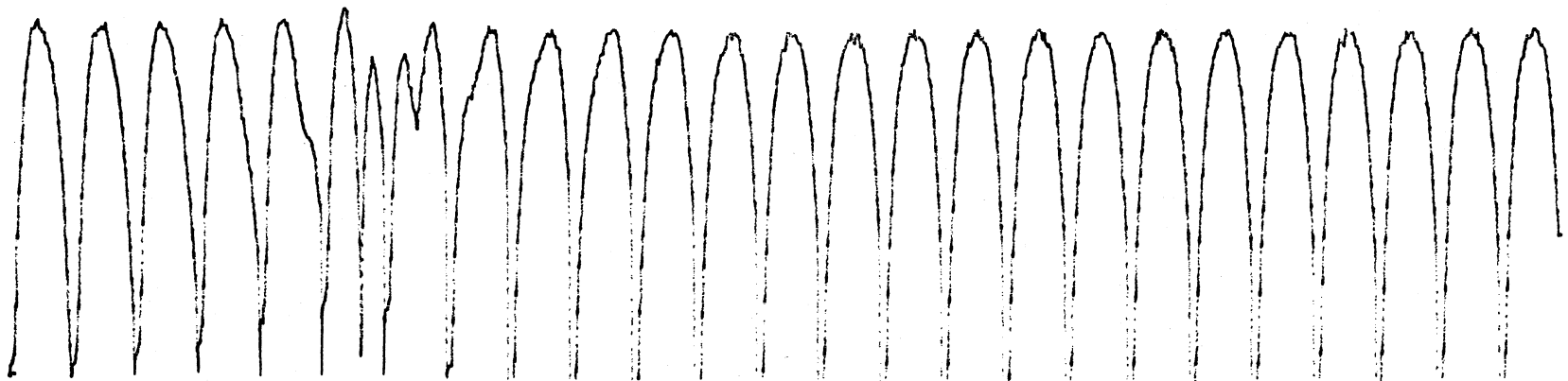
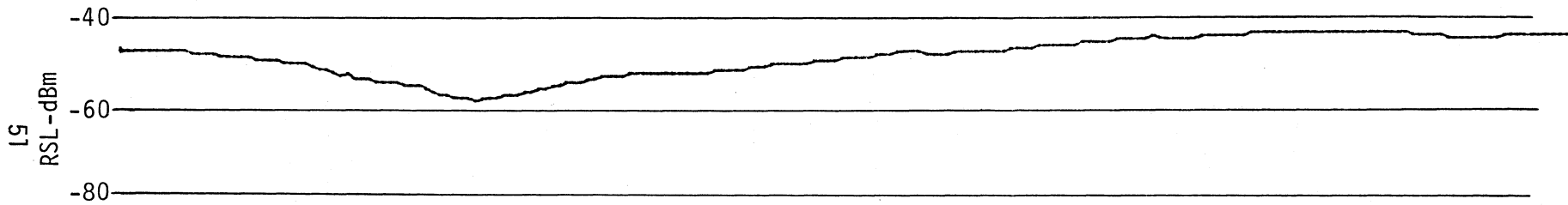
Figure 15. Results of special nondiversity performance measurements performed on 2 September 1981.

2 September 1981
1809:29

1809:54



PMTC Radio



DRAMA Radio

Figure 16. An example of the spectral distortions caused by multipath activity during the special tests conducted on 2 September 1981. The spectral functions were recorded at 1 s intervals.

The space-diversity improvement factors calculated here (for both radios) are higher than one would calculate for similar data obtained by Barnett (1978) and Anderson et al. (1978). The latter measurements were made over paths considerably shorter (42.5 km and 51 km, respectively), and Barnett's data were for a 6 GHz system. Based on the measured data during the nondiversity tests at PMTC, the multipath environment was such that the same order of magnitude of errored-seconds could occur in a few hours that Barnett observed in 25 days of testing. For these reasons, it is probably inappropriate to compare results further.

The two space diversity improvement factors calculated here differ by about the same factor that was previously calculated from the data of Table 7. Both comparisons indicate that the PMTC switch combiner performed better by a factor of 1.2 to 1.3 than that implemented for the DRAMA radio.

The second test shown in Figure 15 was the same as the first, but with both radios switched to a nondiversity configuration on the upper antenna. This test was conducted from 1845 to 2000 Z. The results are quite different from those of the first test on the low antenna. The high antenna performance level is slightly lower for the DRAMA radio, but a drastic change in level is seen for the PMTC radio. An analysis of the multipath data during this test showed a nominal delay of 12 ns which translates to a 48% effective frequency diversity. The low performance values for the PMTC radio suggested that the multipath is affecting this frequency much more severely. This is verified from the spectral plots shown in Figure 17, where the frequency selective distortion to the PMTC spectra is seen to be very severe and persistent. In this case, the disparate performance due to the frequency diversity precludes the test from being used for further evaluation of the space-diversity performance. The calculated frequency diversity improvement factor is approximately 3.

For the final test in the series, the configuration was changed for operation on the lower diversity antenna (as in the first test), but the AE on the PMTC receiver was again turned on. As seen in the plotted data (Fig. 15), the non-diversity performance for the DRAMA radio had improved with respect to the first test. The refractivity data of Figure 11 show that the elevation of the layer was moving downward, and the 2259 Z sounding places it about 50 m lower than it was during the first test. The later elevation is about 515 m, which would yield a multipath delay on the order of 6 ns. This value has been confirmed from the impulse response data, and it corresponds to a 31% frequency diversity factor as compared to the 90% factor during the first test. The result is that the non-diversity performance between the two test periods has changed so much that a

2 September 1981
1850:37Z

1850:42Z

1850:47Z

1850:52Z

1851:17Z

PMTc SPECTRA - High Antenna

53

DRAMA SPECTRA - High Antenna

Figure 17. A sample of the received signal spectra measured from both radios during the nondiversity test on the upper antenna (Figure 15). Note a gap in the record, indicating that the DRAMA radio registered no error or alarm data between 1850:57Z and 1851:17Z.

reference for use in evaluating the improvement due to the AE in the PMTC system is lost. Again we find that this factor has eluded us, and must await the more detailed analyses of the error distribution data.

The results of these special tests illustrate a basic problem that can develop when quantitative results are sought from measurements made sequentially in time. The preferred test arrangement in any dynamic environment would make use of simultaneous measurements for different system configurations. Future tests being planned for the DRAMA radio on the PMTC link will provide the capability for parallel configuration tests.

7. SUMMARY AND CONCLUSIONS

This report describes a comprehensive test program, in which the performance of digital microwave radios was measured over an LOS link that is subject to very strong multipath propagation. The initial objective of the program was to evaluate the performance of a commercial radio for the Pacific Missile Test Center (PMTC) over a crucial link in the range communication/data system. The PMTC radio operates at a T3 mission bit rate (44.7 Mb/s) in an 8-PSK mode in the 7-GHz band. This radio had been purchased and installed on a PMTC link, and configured for space diversity. Earlier multipath measurements performed by ITS (Hubbard, 1979) had concluded that this system might require a quad-diversity (frequency and space) configuration to meet the PMTC transmission reliability requirements. In order to determine how the system would actually perform in a multipath environment, a space diversity configuration was established, using the existing facilities for an analog radio. The digital radio was then dedicated to a test mode for this program.

The ITS was tasked to design the test procedures and data acquisition systems. To augment the experiment, the ITS Channel Probe was installed over the same diversity paths (multiplexed with the test radio), so that a direct measure of the multipath conditions could be obtained simultaneously with the radio performance data. In addition, the pertinent meteorological data for the microwave channel were furnished by the PMTC Geophysics Division and were used to correlate the propagation conditions. The report provides a number of examples of how these various measures relate to each other.

The basic measure of performance for the radio was selected to be that of an errored-second. However, a more detailed set of error data were acquired through the use of a burst-error distribution analyzer. The details of these data are given in Sections 3 and 4 of this report. Section 3 presents a description of all

measured data. Section 4 discusses how the data were recorded in the various data acquisition systems.

Analyses of all of the acquired data have not been performed at the date of this report. The PMTC personnel have analyzed some of the data, but the results are not yet available. Section 5 of the report presents the details of the data formatting and the processing routines that will be followed in the error analyses. It should be noted that these data include a rather complete and dynamic compilation of system status and alarm signals. Examples of these data, and the methods used to both record and evaluate them, are presented in Section 5.

During the conduct of the PMTC program, the ITS was tasked by the U.S. Air Force (Electronic Systems Command) to test the performance of a military digital microwave radio for its susceptibility to multipath. This radio is being procured under the Digital Radio and Multiplex Acquisition (DRAMA) program, and it is commonly referred to as the DRAMA radio. During the late summer and fall months of 1981, the DRAMA radio was added to the PMTC test configuration. It was multiplexed into the same space diversity channels on the test link. The installation provided a means for testing the performance of both radios in exactly the same transmission channels, and the same multipath conditions. The only difference in configuration was the frequency of operation.

Since the detailed performance data (error distribution) have not been analyzed for the PMTC radio, the results contained in this report are limited to comparative performance between the two radio systems. Several special periods of time were analyzed on the basis of errored-second data only. The results are summarized as follows:

1. During periods of full diversity operation, the PMTC radio performed better than the DRAMA system by a factor of 1.18. This relative factor was found to be the same during different multipath delay conditions.
2. The result in 1 above was also found when the adaptive equalizers in the PMTC radio were inactive. It was therefore concluded that the improvement was essentially due to differences in the switched-combiner algorithms. This result also precluded any evaluation of the adaptive equalizers based on the errored-second data.

3. Improvement factors for each radio were derived, comparing the space diversity performance with a short test of nondiversity performance. The following results were found:

Space Diversity Improvement Factors

PMTIC Radio : 1.54

DRAMA Radio: 1.17.

These results, when compared with each other, also indicate an improvement on the order of 1.3 for the diversity switch in the PMTC radio.

4. Nondiversity comparative data were somewhat inconclusive because of the frequency diversity formed in the data. Based on very short test periods, the following factors were found:
 - (a) With an effective frequency diversity of 90% (no diversity is equivalent to 100%), the DRAMA radio performed better than the PMTC radio by a factor of 1.1. However, it is shown in the text that the multipath effects favored the DRAMA frequency.
 - (b) With an effective frequency diversity of 48% (nearly ideal), the DRAMA radio performed better than the PMTC radio by a factor of nearly 3. The corresponding impulse response and signal spectra data again confirmed that the multipath conditions were favorable to the DRAMA frequency. This test result does indicate that for a given multipath condition, the frequency diversity factor can be as high as 3 or greater.

In addition to the above conclusions, the report presents a few examples of how the impulse response data and the meteorological data for the propagation conditions correlate. These are presented in the forms of ray-trace diagrams and graphical solutions of the multipath origins. A relation between the multipath/frequency-selective distortion from a theoretical approach is illustrated and compared with measured results. These findings are used to show the relevant features of the performance data, and to explain differences observed.

8. ACKNOWLEDGEMENTS

The author wishes to acknowledge the following individuals and agencies who made this study possible.

The Range Development Department of PMTC who sponsored the original test program for the PMTC radio. In particular we wish to thank Messrs. Jim Weblemoe and Jim Kaness.

The Range Communications Division at PMTC who supported the project from inception with logistic, technical and personnel support; in particular we thank Messrs. Henry Merhoff, Jim Ordner, and the entire team of individuals who operate the Laguna Peak and San Nicholas Island terminals.

The Digital European Backbone (DEB) Program Office, USAF Electronic Systems Division who sponsored the test phase for the DRAMA radio. We first thank Capt. Jack Muchuzak who initiated the DRAMA program, and secondly we thank his successor, Capt. Robert Trapp, for his continued interest and coordination of the tests.

Finally, we wish to thank all of those at ITS who participated in the project, but in particular, Mr. Lauren Pratt for his valuable assistance in the field and in the laboratory. Mr. Pratt was responsible for the instrumentation used in the experiment, as well as the significant software developed for analyzing the digital data.

9. REFERENCES

- Anderson, C.W., S. Barber, and R. Patel (1978), The effect of selective fading on digital radio, International Communications Conference, Toronto, Canada, June.
- Barnett, W.I. (1978), Measured performance of a high capacity 6 GHz digital radio system, International Communications Conference, Toronto, Ontario, Canada, June.
- Bean, B.R., and E.J. Dutton (1966), Radio meteorology, NBS Monograph 92, March.
- Dougherty, H.T., and W.J. Hartman (1977), Performance of a 400 Mbit/s System Over a Line-of-Sight Path, IEEE Trans. Comm. COM-25, No. 4, April, pp. 427-432.
- Dougherty, H.T., and E.J. Dutton (1981), The role of elevated ducting for radio service and interference fields, NTIA Report 81-69, March. (NTIS Access. No. PB 81-206138.)
- Hartman, P.R., and E.W. Allen (1979), An adaptive equalizer for correction of multipath distortion in a 90 Mb/s 8 PSK system, International Conference on Communications, Boston, MA, Conference Record, Vol. 1, June.
- Hartman, W.J., and D. Smith (1975), Tilting antennas to reduce line-of-sight microwave link fading, Federal Aviation Administration Report No. FAA-RD-75-38, February.
- Hubbard, R.W. (1979), Investigation of digital microwave communications in a strong meteorological ducting environment, NTIA Report 79-24, August. (NTIS Access. PB 301212/AS.)
- Linfield, R.F., R.W. Hubbard, and L.E. Pratt (1976), Transmission channel characterization by impulse response measurements, OT Report 76-96, August. (NTIS Access. No. PB 258577.)
- PMTC (1976), Communications Capability, Capabilities Development Department, Pacific Missile Test Center, Pt. Mugu, California.

APPENDIX

During the latter part of the tests discussed in this report, the military DRAMA radio was added to the experiment configuration. At this time, a second digital data acquisition system was added to accommodate the DRAMA radio data, and other data that were originally recorded on the analog system. The purpose of this appendix is to present a description of the DRAMA data system, and the formatting methods. The information given here may be compared with that of Sections 4 and 5 to glean the differences between the two digital systems.

The DRAMA data system was essentially the same as that shown in the block diagram of Figure 1 (Section 4). The principal difference was the sampling arrangement used in the computer for the A/D data channels. A variable sampling rate was used for the DRAMA data so that the channel probe impulse signals and all of the spectral data for the radio receivers could be recorded in a digital format. These signals were originally recorded on analog tape.

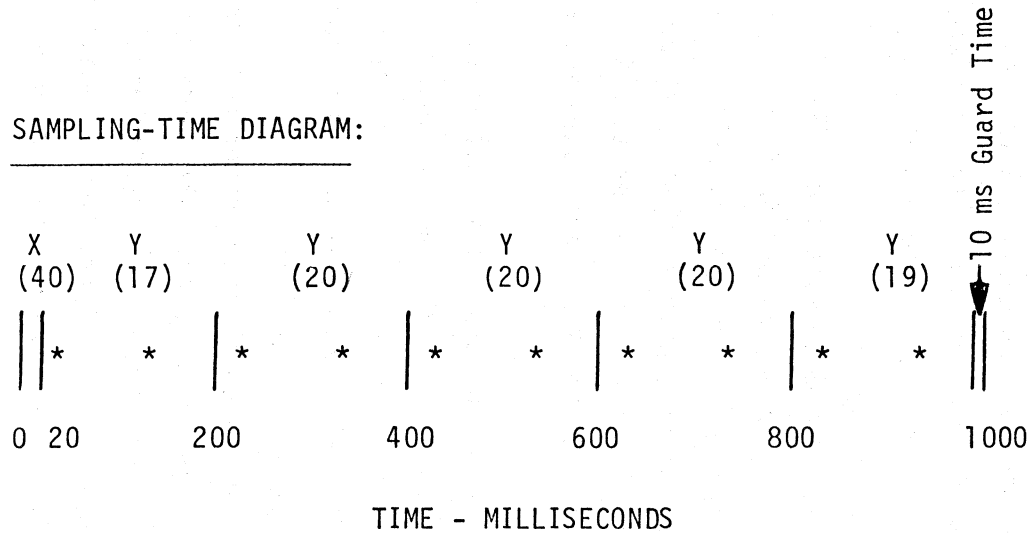
Table A-1 shows the timing diagram for the data sampling. The data were acquired in 1-s blocks, with 5 blocks making up one record or file. The first 20 ms of each second were used to sample the impulse response data, using a 2-kHz sampling rate. The following 970 ms included the spectral data samples at a 100-Hz rate, interspersed with the remaining A/D channels that were sampled at a 10-Hz rate. A 10-ms guard time was used at the end of each block to reset sampling clocks prior to the next data block.

A complete record, consisting of five 1-s blocks was formatted as shown at the bottom of Table A-1. In this way, the records were the same as those for the PMTC radio data in format, and they can be readily synchronized in the analysis procedures. The status and alarm signals were recorded in the same manner as described in Section 4, using a 16-bit I/O interface board.

The performance data were recorded from a synchronous errored-second instrument (Tau-Tron Model S-5000), which provided two outputs. The first is a record of each errored-second (complete with time of occurrence) and the total number of bit errors in each. This output also included a registry for two event markers/counters and a single analog channel. The analog channel was not used. The second output is a periodic summary of the errored-second data, where the period could be selected for 1 min., 15 min., 1 hour, or 24 hours. This registry was a two-line output which included the totals of all the digital entries of each errored-second, the two event counters, and an auxiliary counter that does not register in the interval data. An example of both outputs is shown in Figure A-1. The first is labeled as auto print, and the second as a periodic print.

Table A-1. Digital Data Acquisition System - DRAMA Radio

SAMPLING-TIME DIAGRAM:

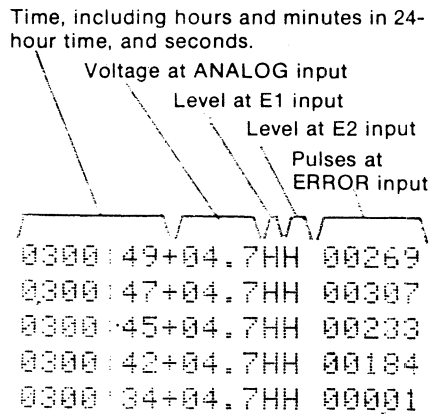


LEGEND:

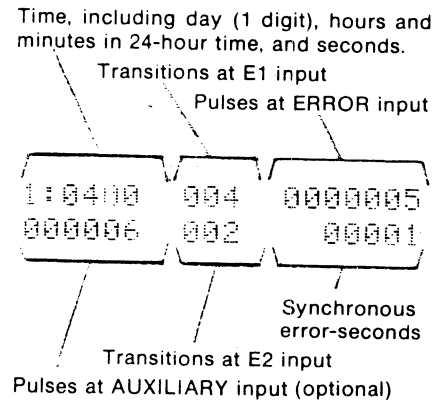
- X - 4 CHANNELS @ 2 kHz (IMPULSE RESPONSE DATA) - 40 samples/s/channel
- Y - 4 CHANNELS @ 100 Hz (SPECTRAL DATA) - 96 samples/s/channel
- * - 8 CHANNELS @ 10 Hz (RSL AND OTHER ANALOG SIGNALS) - 10 samples/s/channel

DATA RECORD FORMAT:

- 1 - DATE AND TIME OF DAY
- 2 - 5 SECONDS OF A/D SIGNAL DATA
- 3 - 16 BIT I/O STATUS AND ALARM SIGNALS (Sampled at 0.1 s intervals)
- 4 - SYNCHRONOUS ERRORED-SECOND DATA
 - Time of day
 - Total No. of Errors
 - Event Counters



(a) Auto Print



(b) Periodic Print

Figure A-1. An example of the errored-second performance data as they appear in the printer output record.

The example of error/event data in Figure A-1 is shown as it would appear on a paper printer. An interface card was built in the ITS laboratories that converted the ASCII coded data in these registers to a serial stream, and they were then buffered into the computer for recording on the digital magnetic tapes in the same format as shown.

The event counters function differently. The channel marked E1 in Figure A-1 registers either a high (H), low (L) or activity (A). The latter indicates that more than one event took place during the 1-s interval, but the count is not known. The channel marked as E2 operates in the same manner, with the exception that activity within the second is counted up to 9. Counts greater than 9 are indicated by a ? in the ASCII code.

Channel E1 was used to register the receiver switches in the diversity combiner of the radio. Channel E2 was used to indicate the loss of frame sync alarm in the DRAMA system, which includes entries from both receivers. The auxiliary channel was used to count the number of times that the $BER > 10^{-3}$ alarm was turned on in a given periodic interval. All of the acquired data used a periodic setting of either 1 min. or 15 min., depending on the error activity at the time.

A complete list of all of the DRAMA radio signals is given in Table A-2. The status data were recorded as a 16-bit parallel word (as described in Section 4), and are decoded from the octal record as illustrated in Section 5.

Table A-2. DRAMA Radio Data Signals

Analog Signals:

- Received Signal Level (RSL) - Receiver A
- Received Signal Level (RSL) - Receiver B
- Signal Quality Voltage - Receiver A
- Signal Quality Voltage - Receiver B
- Received Signal Spectrum - Receiver A
- Received Signal Spectrum - Receiver B

Digital Status and Alarm Signals:

- Loss of Data or Clock
- Loss of Frame Sync
- $BER > 10^{-3}$ (Estimated from frame error data)
- Receiver A On-line
- Receiver B On-line
- Receiver Switch - Manual/Auto
- Receiver Timing Alarm
- Receiver A Alarm
- Receiver B Alarm

Digital Data Performance:

- Errored-Seconds (No. of errors in each)
- Event Counters
 - E1 - Diversity Receiver Switches
 - E2 - Loss of Frame Sync
 - AUX - $BER > 10^{-3}$ Alarm

BIBLIOGRAPHIC DATA SHEET

1. PUBLICATION NO. NTIA Report 83-126		2. Gov't Accession No.	3. Recipient's Accession No.
4. TITLE AND SUBTITLE DIGITAL MICROWAVE TRANSMISSION TESTS AT THE PACIFIC MISSILE TEST CENTER, PT. MUGU, CALIFORNIA		5. Publication Date June 1983	
7. AUTHOR(S) R.W. Hubbard		6. Performing Organization Code NTIA/ITS.N4	
8. PERFORMING ORGANIZATION NAME AND ADDRESS Institute for Telecommunication Sciences National Telecommunications and Information Administration U.S. Department of Commerce, Boulder, Colorado 80303		9. Project/Task/Work Unit No. 9103543	
11. Sponsoring Organization Name and Address Department of the Navy Pacific Missile Test Center Point Mugu, California 93042		10. Contract/Grant No. MIPR N6312680MP31554	
14. SUPPLEMENTARY NOTES		12. Type of Report and Period Covered Technical Report	
15. ABSTRACT (A 200-word or less factual summary of most significant information. If document includes a significant bibliography or literature survey, mention it here.) This report describes an experiment designed to measure the performance of digital microwave radio systems in a line-of-sight (LOS) link that is subject to strong atmospheric multipath. It outlines the measurements made to characterize the propagation medium, the status of space-diversity receiver systems equipped with switched combiners, and the burst error-statistics caused by the multipath environment. The results presented in this report compare the performance of two radios, operating simultaneously in the same transmission channel. Detailed error distribution data have not yet been analyzed.		13.	
16. Key Words (Alphabetical order, separated by semicolons) adaptive equalization; atmospheric multipath; digital communications; impulse response			
17. AVAILABILITY STATEMENT <input checked="" type="checkbox"/> UNLIMITED. <input type="checkbox"/> FOR OFFICIAL DISTRIBUTION.		18. Security Class. (This report) Unclassified	20. Number of pages 76
		19. Security Class. (This page) Unclassified	21. Price:



